NASA TN D-1739

NASA TN D-1739

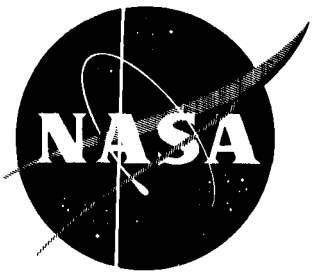

TECHNICAL NOTE

D-1739

COMPATIBILITY OF CESIUM VAPOR WITH SELECTED MATERIALS AT TEMPERATURES TO 1200° F

By Joseph M. Lamberti and Neal T. Saunders

Lewis Research Center
Cleveland, Ohio

NATIONAL AERONAUTICS AND SPACE ADMINISTRATION

WASHINGTON

August 1963

NATIONAL AERONAUTICS AND SPACE ADMINISTRATION

TECHNICAL NOTE D-1739

COMPATIBILITY OF CESIUM VAPOR WITH SELECTED MATERIALS AT TEMPERATURES TO 1200° F

By Joseph M. Lamberti and Neal T. Saunders

SUMMARY

Compatibility studies of cesium vapor with selected materials tested for 48 hours at 500°, 800°, and 1200° F in a cesium vapor atmosphere at pressures of approximately 0.5, 28, and 267 Torr, respectively, are presented. For comparison, control samples were tested under similar conditions of time and temperature in a vacuum of approximately 10^{-6} Torr.

The test materials included the following: refractory metals: tungsten, molybdenum, and tantalum; iron-base alloys: 1020 steel (cold rolled) and type 304 stainless steel; nickel-base alloys: L-nickel, A-nickel, Inconel X, and B-monel; copper-base alloys: copper (electrolytic tough pitch (ETP)), bronze (leaded phosphor bronze), and brass (Muntz metal); precious metals: platinum, gold, and silver; light metals: aluminum (Alclad 24ST) and magnesium; nonmetals: Mycalex, Mykroy, lava, Morganite, and sapphire.

Metallurgical examination indicated that the following tested materials were attacked by cesium vapor to varying degrees: copper, brass, bronze, gold, silver, aluminum, magnesium, Mycalex, Mykroy, and lava.

INTRODUCTION

The alkali metals, group I of the periodic table, include the better known metals lithium (Li), sodium (Na), and potassium (K) and the lesser known metals rubidium (Rb), cesium (Cs), and francium (Fr). As a family of elements, they combine with most nonmetals, displace hydrogen from water and most inorganic acids, and reduce the oxides or chlorides of many metals. Their similar chemical properties are explained by the single electron in the outermost shell of each atom, and the degree of their chemical activity generally follows their position in the electrochemical series: Fr > Cs > Rb > K > Na > Li (refs. 1 and 2). Representative values of the more common physical properties of these metals are listed in table I.

Because of their relatively low ionization potentials (i.e., the work done in removing an electron from an atom), the alkali metals have been considered for use in advanced space-power systems such as electric rockets (refs. 3 and 4). In these systems, thrust is proportional to the mass of the propellant. The pri-

mary emphasis, therefore, has been placed on cesium as a propellant because it has the highest atomic weight (132.91) and the lowest ionization potential (3.87 v) of the stable alkali metals. (Francium has no known stable isotope (ref. 5).) In addition, cesium has also been used in energy-conversion schemes such as the cesium-vapor diode tube (ref. 6) and in power-generation systems using magnetohydrodynamic principles (ref. 7).

As the technology of these systems advanced, it soon became apparent that there was a need for more information on the compatibility of cesium vapor with materials used in the construction and testing of these devices. Although liquid-metal corrosion data are available for the alkali metals (ref. 8), very little has appeared in the chemical and metallurgical literature on the vapor-phase compatibility of these metals, particularly cesium. The reports that have appeared on the effects of cesium on materials (refs. 9 to 13) are qualitative in nature and in disagreement in many areas. Consequently, a preliminary systematic investigation was undertaken at the NASA Lewis Research Center (as a part of the electrostatic-rocket-engine research program) to test several common materials in cesium atmospheres. The test materials included the following:

(1) Refractory metals: tungsten, molybdenum, and tantalum

(2) Iron-base alloys: 1020 steel (cold rolled) and type 304 stainless steel

(3) Nickel-base alloys: L-nickel, A-nickel, Inconel X, and B-monel

(4) Copper-base alloys: copper (electrolytic tough pitch), bronze (leaded phosphor bronze), and brass (Muntz metal)

(5) Precious metals: platinum, gold, and silver

(6) Light metals: aluminum (Alclad 24ST) and magnesium

(7) Nonmetals: Mycalex, Mykroy, lava, Morganite, and sapphire

Samples of each of these materials were tested for 48 hours at 500°, 800°, and 1200° F in cesium-vapor atmospheres at pressures of approximately 0.5, 28, and 267 Torr, respectively. For comparison, control samples were tested under similar conditions of time and temperature in a vacuum of approximately 10^{-6} Torr.

The primary purpose of this study was to screen quickly the gross, short-term effects of cesium vapors on materials at temperatures up to 1200° F. In addition, the materials were metallurgically examined, and, in some cases, the mode of attack was postulated for those that were affected by cesium.

MATERIALS AND APPARATUS

Cesium

The cesium used in this study was supplied in the liquid state from a com-

mercial source to a specification of 99.0-percent minimum purity. A spectrographic analysis of the alkali-metal impurities of a representative sample of this material was as follows:

Impurity	Percent
Rubidium	0.50
Potassium	.40
Sodium	.02
Lithium	.005

An analysis at this laboratory of the oxygen content of the cesium (by the procedure described in refs. 14 and 15) yielded values in the range 0.25 to 0.30 percent. These values, however, must be considered as only an indication of the oxygen content and not as absolute values because the several analytical techniques now in use were originally established for oxygen determinations in sodium (refs. 14 to 16), and their applicability to cesium is not considered completely reliable at the present. Actually, the absolute value of the oxygen content could be as much as a factor of 10 higher than the analyzed values.

To prevent any further contamination, the cesium was supplied and stored in hermetically sealed, Pyrex-glass capsules. It has been reported (ref. 9) that over a long period of time cesium attacks glass by removing oxygen from it, especially at elevated temperatures. The corrosion is negligible, however, under 500° F, and thus oxygen pickup from the glass capsules is considered negligible under these room-temperature storage conditions.

Test Materials

The selected materials used in this study are listed in table II along with their typical composition limits and approximate melting points (from ref. 17). The precious metals (silver, gold, and platinum) were specially procured to a specification of 99.9-percent minimum purity. All the other materials were of standard commercial grade obtained from the stock supply at this Center. The compositions listed in table II, therefore, are merely typical compositions. Since the main purpose of this investigation was to study the effects of cesium vapor on common materials, no attempt was made to control the composition and purity of the test materials.

Test Apparatus

The tests were conducted in a stainless-steel, cylindrical, vacuum chamber (fig. 1) that was 3.8 inches in diameter and 13.3 inches long (inside dimensions). The specimens were supported in the test chamber by a removable specimen rack that kept the samples separated during the test. A cesium ampoule was suspended above the specimen rack along with a bellows-type mechanical plunger that was used to break the ampoule at the start of the test phase. The entire test chamber was anchored in an electrically heated muffle furnace, and the temperature distribution within the chamber was monitored by a series of thermocouples

held in a thermocouple probe.

A vacuum pumping system was connected to one end of the test chamber, and a butterfly-valve (damper-type) assembly was located at the mouth of the test chamber to restrict the cesium vapor to the test area. The vacuum pumping system (consisting of a mechanical forepump, an oil diffusion pump, and a liquid-nitrogen cold trap) was capable of reducing the pressure in the test chamber to approximately 10^{-6} Torr. After the test system was evacuated to 8×10^{-6} Torr, heated, and isolated from the vacuum pumping system, the overall pressure rise was measured. This pressure rise is plotted in figure 2.

In order to determine approximately the outgassing rate of the stainless-steel chamber used in this investigation, the following equation was used:

$$\text{Outgassing rate} = \left(\frac{1}{A_s}\right)\left(\frac{V}{1000}\right)\left(\frac{1}{3600}\right)\left(\frac{\Delta P}{\Delta t}\right) \qquad \text{(mm Hg)(liters)/(sec)(sq cm)}$$

or

$$\text{Outgassing rate} = (2.78\times10^{-7})\left(\frac{V}{A_s}\right)\left(\frac{\Delta P}{\Delta t}\right) \qquad \text{(mm Hg)(liters)/(sec)(sq cm)}$$

where

A_s surface area, sq cm

$\left(\frac{V}{1000}\right)$ volume, cu cm

$\left(\frac{\Delta P}{\Delta t}\right)$ rate of pressure rise, mm Hg/hr

For the time (48 hr) and the chamber size (volume, 6088.3 cu cm; surface area, 2515.9 sq cm) of this investigation, the outgassing rates at 500°, 800°, and 1200° F were 2.0×10^{-9}, 2.5×10^{-8}, and 8.0×10^{-8} (Torr)(liter)/(sec)(sq cm), respectively. The measured value for stainless steel at 25° C is 8×10^{-9} (Torr)(liter)(sec)(sq cm) (ref. 18). Since there are many factors involved in determining outgassing rates of various materials under different conditions, no attempt was made to extrapolate the value for 25° C to the test temperatures. Consequently, it was assumed that evolving gases that had been absorbed in the stainless-steel walls of the chamber accounted for the pressure rise in figure 2. The actual leak rate of the system, therefore, must have been low and probably had only a minimum effect on the test conditions.

Cesium Handling

The cesium capsules used in the tests were approximately 2.5 inches long and 0.5 inch in diameter. Prior to being filled with cesium, each capsule was washed thoroughly with a detergent and immersed in hot chromic acid for several

hours. After several rinsings with distilled water and ethyl alcohol, the capsule was dried in an oven and weighed. By means of a stainless-steel, vacuum-tight adaptor, the capsule was attached to a laboratory-bench vacuum system (consisting of a small mechanical forepump and a mercury diffusion pump) and evacuated to 10^{-4} Torr. During the evacuation, the capsule was heated with an infrared heating light placed close to the glass ampoule. The small valve of the adaptor was closed, and the entire assembly, with the evacuated capsule, was removed from the vacuum train and placed in a dry box.

The dry box, an airtight rectangular chamber of stainless steel, was purged with purified and dried helium. Access to the inside of the box was possible by means of rubber gloves securely fastened to port holes. Prior to any cesium transfer, small getter ampoules of cesium were purposely broken in the chamber to ensure that all the detectable oxygen was removed. After the adaptor was removed, the capsule was filled with the desired amount of cesium by means of a hypodermic syringe with a stainless-steel needle. The closed adaptor was placed on the filled capsule, and the entire assembly was removed to the vacuum train for evacuation to 10^{-4} Torr. The capsules were sealed while still attached to the vacuum system. The difference between the weighed empty capsule and the evacuated cesium-filled capsule gave the net amount of cesium in each capsule.

Sample Preparation and Testing

The specimen samples, approximately 2.5 inches long and 1 inch wide and varying in thickness from 0.25 to 0.015 inch, were buffed to a dull luster to remove any scratches on the surfaces and cleaned with acetone and ethyl alcohol to remove any organic films. For expediency, several materials were tested in each run. Samples of the materials were suspended in the specimen rack and placed in the test chamber. The butterfly valve and the vacuum valve were left open while the test chamber was evacuated to approximately 10^{-6} Torr and subsequently heated to the desired test temperature. Pumping was continued for about 12 hours with the chamber at temperature in an attempt to minimize the effects of chamber outgassing. The vacuum valve and damper valve were both closed before the cesium capsule was broken.

After the run was completed, the test chamber and contents were allowed to cool slowly to room temperature, and helium was subsequently bled into the system. The chamber was transferred to the dry box, where it was opened, and the samples were removed. The samples were then washed with anhydrous ethyl alcohol and placed in a desiccator. Rarely was any cesium found beyond the damper valve or in the liquid-nitrogen cold trap. The fact that most of the cesium was found in the vicinity of the specimens indicated that the damper valve was effective in containing the cesium vapor and that pressures near the calculated values probably existed in the test chamber during the test.

For comparison, samples identical to those tested in cesium were subjected to the same temperatures in a static vacuum of about 10^{-6} Torr. Procedures were similar to those used in the cesium tests except that the cesium capsule was not broken. This test was performed in order to differentiate between cesium and thermal effects on the test samples.

Cesium Pressure

The amount of cesium used was governed by the size of the ampoule that would fit in the apparatus. The maximum amount that could be contained was approximately 4 grams, and this amount of cesium was used in each of the test runs. Since there was no gage to measure the pressure in the cesium atmosphere, the pressures of cesium at 500° and 800° F were established by its vapor pressure; they were 0.5 and 28 Torr, respectively (ref. 19). At 1200° F, however, 4 grams of cesium were not sufficient to maintain a vapor-liquid equilibrium with the metal in the test chamber. If it is assumed that all the cesium had vaporized and that it is a monatomic gas that obeys the ideal gas laws, the calculated cesium pressure at 1200° F is 267 Torr.

Metallographic Examination

Metallographic specimens were sectioned from each test sample with a water-cooled cutoff saw. Water cooling was used to minimize the effects of cutting on the cross sections of the samples. The specimens were mounted individually in either Bakelite or Hysol with the cross sections visible. The selection of the mounting material depended on the hardness of the test material in the "as-received" state. The same mounting material was used for all samples of each test material, however. The mounted specimens were polished, etched, examined, and photographed by the application of metallographic techniques conventionally used for each of the materials.

Rockwell hardness tests were made on the surfaces of most of the metallic test samples. These measurements were made on the sections not utilized for metallographic study. The samples of some of the test materials (tantalum and the precious metals) were too thin to obtain reliable surface-hardness readings; therefore, the Rockwell hardness tests were omitted for these materials.

Microhardness tests were made with the Vickers diamond-pyramid indentor on the cross sections of all the metallic specimens. These tests were performed on the mounted specimens after the metallographic examination was completed. Because hardness measurements were difficult to make with the nonmetals, these measurements were not obtained for any of these materials.

FACTORS IN INTERPRETATION OF RESULTS

Sample Contamination

Ideally, each material should have been tested by itself in order to determine the actual influence of cesium vapor, and, in addition, extremely high-purity materials should have been used. For expediency in this test series and to simulate operating conditions more nearly, however, several commercial-grade materials were grouped together and tested simultaneously. Because of this simultaneous testing, many of the observed effects of the test conditions were probably biased by cross contamination from neighboring samples.

Oxygen Contamination

The role of oxygen must be given serious consideration in any gas-phase compatibility study, and particularly with the use of cesium since it has a high affinity for oxygen. In this series of tests, several sources were available to supply oxygen to the metal-cesium interface; namely, residue oxygen present in the vacuum system, oxides in the cesium, outgassing of the test chamber, cross contamination, or the test material itself. Comparison of the negative free energies of metal oxides with that of cesium oxide (see ref. 20) indicates the stability and probability of various metal oxides forming in a cesium atmosphere with oxygen present. In most cases, cesium has a much greater affinity for oxygen than do the constituents of the test materials; thus, oxide coatings or inclusions in the test material were probably reduced by cesium. This is really not the effect of cesium on a pure material, however, but rather the reaction of cesium with oxygen.

Effects of Temperature

In a study of this type, the test temperature could appreciably alter the structure of the test materials. Such temperature effects as phase transformations, changing solubility limits, and increased diffusion rates all add to the difficulty of interpreting the test results. The use of duplicate samples subjected to similar temperature conditions in cesium and in vacuo helped to distinguish between the results of cesium effects and temperature effects.

RESULTS AND DISCUSSION

Refractory Metals

Tungsten and molybdenum. - Results of the metallurgical examination of the samples of these metals did not reveal any appreciable change as a result of the various test conditions. This is shown in the microstructures of the cesium- and vacuum-treated samples that are compared to those of the as-received samples in figure 3 for tungsten and figure 4 for molybdenum. The Rockwell hardness and microhardness data for these and all other test samples are summarized in tables III and IV, respectively. The hardness values for both tungsten and molybdenum tend to confirm the metallographic observations since no appreciable change in hardness of samples of these materials resulted from any of the test conditions.

Tantalum. - A tarnishing effect was noticed on all tantalum samples tested. Since the same results were observed on both cesium- and vacuum-treated samples, this tarnishing is not considered to be a result of cesium corrosion but, more likely, a result of oxidation of the surface by the oxygen present in the test atmosphere.

Examination of the microstructures (fig. 5) and microhardnesses (table IV) of the samples tested at 500° and 800° F compared with those of the as-received samples failed to reveal any appreciable differences resulting from the test conditions. The samples tested at 1200° F, however, demonstrated more than a two-

fold increase in microhardness over those of the samples tested at lower temperatures. The microstructure of the 1200° F cesium-treated sample (fig. 5(g)) was much cleaner and freer of inclusions than those of the other samples; however, the similarly tested vacuum-treated sample (fig. 5(d)) demonstrated a dark needlelike structure similar to that found in hydrogen-embrittled tantalum (ref. 21). This embrittlement probably resulted from the presence of hydrogen in the test system supplied by the outgassing of nearby test samples and/or the test system. The embrittlement was not as severe in the cesium tests because the higher pressure of this atmosphere tended to reduce the amount of outgassing. The increased hardness of both samples tested at 1200° F, however, is considered to be due to the increased solubility of hydrogen and the higher diffusion rates at this temperature.

It is thus concluded from these tests that tantalum is probably not greatly affected by pure cesium up to 1200° F, but that even very small quantities of hydrogen in the cesium atmosphere may cause drastic changes in the structure and resultant properties during elevated-temperature operations. Since tantalum allows relatively large solubility of other interstitial elements, such as oxygen and nitrogen, it is quite possible that small quantities of these elements in the operating atmosphere may also adversely affect tantalum.

Iron-Base Alloys

1020 Steel (cold rolled). - This material exhibited excellent resistance to cesium attack, but other effects were noted. The surfaces of the samples were tarnished as a result of testing in both cesium and vacuum. This tarnishing resembled light rusting commonly found in this type of material and was probably due to surface oxidation from the oxygen in the cesium and/or from that vaporized out of nearby samples. No appreciable change was observed in the microstructure (fig. 6) or the hardness data (tables III and IV) for the samples tested at 500° and 800° F. Both the microstructures and hardnesses of the vacuum- and cesium-treated samples were appreciably affected, however, by the test temperature of 1200° F. This test temperature actually subjected the material to a softening, spheroidizing anneal (i.e., the carbide precipitates formed into very small spheres that could only be resolved at high magnifications). Thus, the highest temperatures removed all strengthening effects of prior heat treatments and cold work, but the test atmosphere had no appreciable effect on this material.

Type 304 stainless steel. - As in the case of 1020 steel, slight tarnishing of the surfaces was observed in samples tested at 800° and 1200° F in both vacuum and cesium atmospheres. Again, this is believed to be the result of vaporization of impurities from nearby samples in the test chamber. Comparison of the microstructures of the 1200° F samples with those of the samples subjected to lower temperatures (see fig. 7) indicates that the highest test temperature also caused recrystallization of this material. Note that most of the effects of prior working were removed by the 1200° F heat treatment. The irregular surfaces in most of the photomicrographs indicate that some of the alloying constituents probably vaporized from these samples. Cesium, however, apparently had no adverse effects on the samples of this material.

Nickel-Base Alloys

L-nickel. - The samples of this material demonstrated a gradual decrease in hardness with increasing test temperature, as indicated in the data of tables III and IV; the largest difference, a decrease of 10 points on the Rockwell C scale, occurred between 800° and 1200° F. The change in microstructure accompanying this softening is shown in figure 8. Increasing the test temperature apparently resulted in solution of some of the original grain-boundary precipitates. Since similar results were observed in both vacuum- and cesium-treated samples, it is concluded that L-nickel is not adversely affected by cesium.

A-nickel. - The composition of this material is similar to that of L-nickel except that A-nickel contains slightly larger amounts of the alloying elements carbon, iron, and copper. A-nickel was also expected to be resistant to cesium attack, therefore, but to be affected by the test temperature under these test conditions. This was found to be true and is demonstrated in the photomicrographs of figure 9 by the similar solution of precipitates; in addition, slight grain growth and narrow, fine-grained surface layers are apparent. These effects seem greater in the vacuum-treated samples than in those exposed to cesium. The hardness values in tables III and IV confirm the latter observation since the vacuum-treated samples were all softer than the corresponding cesium-treated samples. In addition, the hardness apparently decreased with increasing test temperature, as expected with this type of material.

The hardness changes and fine-grained surface layers were believed due to vaporization of some of the minor alloying constituents of the A-nickel. The discrepancy in hardness between comparable cesium and vacuum tests was probably due to the difference in pressure in the test atmospheres; that is, the low pressures in the vacuum tests allowed greater vaporization than was allowed in the higher pressure cesium tests. Since similar effects were noted in both cesium and vacuum tests, it is concluded that cesium itself is probably compatible with A-nickel. It is quite possible that prolonged use of A-nickel in vacuum or any low-pressure atmosphere, however, may result in loss of strength to levels possibly below the design criteria.

Inconel X. - This material differs from the previous nickel-base materials in that it depends on the precipitation of complex intermetallic compounds (primarily carbides) for its high-temperature strength. These precipitates are quite evident in the structures demonstrated in the photomicrographs of figure 10. These photomicrographs indicate that the precipitates were present within the grains and also at the grain boundaries of the samples. In many instances, the precipitates outline the location of grain boundaries that were present at some prior time in the fabrication history of the material. The photomicrographs of figure 10 show essentially no change in microstructure, however, as a result of any of the test conditions. With this observation, plus the fact that the hardnesses of the samples were not greatly affected by the test conditions, it is concluded that cesium did not attack the Inconel-X samples in this series of tests.

B-monel. - The microstructures of samples of this material (fig. 11) demonstrate a fine-grained surface layer similar to those found in the L-nickel and

A-nickel samples previously described. This zone was also probably due to vaporization of some of the minor alloying constituents from the grains near the surface. Since the hardness values (tables III and IV) were not appreciably affected by the test conditions and similar results were exhibited in both cesium- and vacuum-treated samples, it is concluded that cesium had no adverse effects on B-monel under these test conditions.

Copper-Base Alloys

Copper (electrolytic tough pitch, ETP). - The photomicrographs (fig. 12) of the test samples of this material indicate that both test temperature and cesium affected the material. The effect of temperature on grain growth is quite evident, particularly when the test temperature is increased from 800° to 1200° F. Subjection of samples of this copper to a cesium atmosphere apparently resulted in the formation of a layer of fine grains at the exposed surfaces. This layer is quite evident in the 1200° F, cesium-treated sample (fig. 12(g)). The Rockwell surface-hardness readings (table III) confirm this result since the values for the cesium-treated samples were consistently lower than those of the comparable vacuum-treated samples.

The apparent cesium attack of copper may have been partly due to the oxygen impurity of the test system previously mentioned. It may also have been due to the oxygen content of the copper itself (0.04 percent); that is, the strong affinity of cesium for oxygen might have reduced any oxides present near the surface of the test samples. It has previously been reported (ref. 12) that oxygen-free copper withstands cesium attack at 500° F, but normal copper (with oxide inclusions) deteriorates rapidly under similar conditions. Oxygen-free copper, therefore, may allow use of copper components in cesium atmospheres to a greater extent than now seems possible with standard commercial copper. Electrolytic (ETP) copper may even be usable in the lower temperature range; a sample of this material subjected to a cesium atmosphere at 500° F for 200 hours in an additional test exhibited no worse effects than those observed in samples that ran for 48 hours in this series of tests (fig. 12(e)).

Bronze (leaded phosphor bronze). - This copper-base material also appeared to be slightly affected by the cesium atmosphere, as evidenced by the photomicrographs of figure 13. Note that both the 800° and 1200° F cesium-treated samples exhibited irregular surfaces. This is probably the result of a reaction similar to that observed with the previous copper samples; that is, reduction of the surface oxides by the cesium atmosphere. The large decrease in hardness (table III) noted in the 800° and 1200° F cesium tests is probably only a temperature effect since a corresponding decrease in hardness was also noted in the comparable vacuum-treated samples. In fact, this thermal softening effect was even greater in the vacuum-treated samples, probably because of the increased vaporization rate of the tin-rich phase in the lower pressure atmosphere. Since the effect of cesium on these samples is relatively small, this material (like ETP copper) may possibly be used in future cesium applications, for at least short durations, if the quality of the material is closely controlled.

Brass (yellow, Muntz metal). - The effect of temperature on this material is

demonstrated quite vividly in the photomicrographs of figure 14. It can be seen that increasing the test temperature caused an increasing amount of intergranular attack. Much of this attack is merely due to dezincification (i.e., diffusion and vaporization of the low-melting, zinc-rich phase). In addition to the thermal effects, though, there must have been some cesium attack of the samples since the loss of the zinc phase appears greater in the cesium-treated samples despite the higher pressure of the test atmosphere. In addition, the hardness (table III) of the cesium-treated sample is greater than that of the corresponding vacuum-treated sample. Cesium, then, must have preferentially attacked the second phase, and possibly formed a compound of cesium and zinc, as it traversed the grain boundaries of the sample. Thus, for any application involving cesium, or even low pressures, this type of brass is unacceptable.

Precious Metals

Platinum. - The photomicrographs of figure 15 indicate that the test conditions used in this study did not have any appreciable adverse effects on platinum. The microhardness data in table IV also indicate no gross changes. Since other studies (ref. 9) have indicated cesium attack of platinum under more severe test conditions, it is quite possible that higher temperature and/or longer test durations could result in substantial cesium corrosion.

Gold. - References 1 and 2 indicate that cesium forms a series of solid solutions with gold; therefore, attack of the gold samples under these test conditions could be expected. These expectations were confirmed by both visual and metallographic examination of the samples. All the cesium-treated samples possessed a dull, powdery surface layer; the 800° F sample showed the worst corrosion. The photomicrographs (fig. 16) of these samples show the extreme grain growth due to temperature effects and the results of surface attack by cesium. The attack appears greater at 500° and 800° F than at 1200° F. This apparent anomaly is possibly due to the lower rate of adsorption and/or the higher solubility limits in gold at 1200° F.

Silver. - Since silver is also known to alloy with other group I elements (refs. 1 and 2), cesium attack might also be expected with this material. As with the gold samples, grain-boundary attack and grain growth increased as a function of increasing test temperature (fig. 17). The deterioration of the grain boundaries is quite evident in the 800° F, cesium-treated sample (fig. 17(f)), and apparently a second phase has formed in the 1200° F samples (fig. 17(g)). Note also that the 1200° F, vacuum-treated sample (fig. 17(d)) shows evidence of vaporization from the areas surrounding the surface grain boundaries. The relatively high vapor pressure of silver at this temperature could be detrimental to the use of silver for long durations in low-pressure atmospheres.

Light Metals

Aluminum (Alclad 24ST). - The results of this series of tests indicate that this aluminum alloy is unusable in a cesium atmosphere above 500° F (see fig. 18). The Alclad-aluminum samples exhibited considerable reaction with cesium at

800° F (fig. 18(e)) with the presence of three distinct surface zones. Microhardness values of each of these zones exhibited a large gradient in hardness. Note that the alloy core seems more prone to attack than the unalloyed cladding. Attempts to run samples at 1200° F resulted in incipient melting, and thus the results were disregarded.

As was the case with several of the previously discussed materials, oxygen impurities in the cesium may account for the corrosive effect of cesium on aluminum. Since aluminum has a greater affinity for oxygen than does cesium, it is quite probable that aluminum reduces any of the cesium oxide present in the atmosphere.

Magnesium. - Only two samples of magnesium were tested; these tests were at 500° and 800° F in a cesium atmosphere. Both samples exhibited such severe grain-boundary attack (fig. 19) that the testing was discontinued. Since magnesium has a low melting point, a high vapor pressure, and an apparent incompatibility with cesium, it is definitely not recommended for use in atmospheres of this type.

Nonmetals

Mycalex and Mykroy. - These two commercially available compounds are representative examples of glass-bonded mica composites that are used as electrical insulators. Temperature effects were very pronounced on both materials. As the test temperature increased from 500° to 1200° F, surface discoloration and erosion resulted. Photomicrographs of the structures of these samples are shown in figures 20 and 21. The Mycalex samples tested at 1200° F laminated and had the appearance of the gross porosity in figures 20(d) and (g). Evidently the materials were tested above their useful working temperatures.

Since the surfaces of each of the cesium-treated samples appear rougher than those of the corresponding vacuum-treated samples, it is assumed that cesium affects these materials. Because these composites are a mixture of various silicates of sodium, calcium, magnesium, aluminum, and so forth, the corrosive effect of cesium may be explained by its reactivity with these various compounds.

Lava. - This material is primarily composed of magnesium silicate and is often used as an electrical insulator. The structures shown in figure 22 indicate that this compound is not compatible with cesium since even the body of the material seems adversely affected by the cesium tests, particularly at 1200° F.

Morganite and sapphire. - These materials are composed of aluminum oxide and are also considered for use as electrical insulators in proposed space engines. There was no apparent effect of the cesium on either of the materials. This apparent compatibility is explained by the fact that aluminum oxide has greater thermodynamic stability than cesium oxide (see ref. 19).

CONCLUDING REMARKS

When the compatibility results are applied to the selection of useful mate-

tant of these factors are operating temperature and time. Many of the materials that exhibited reactions in this study are not necessarily ruled out for use at lower temperatures or for shorter times. Conversely, those materials that appeared compatible with cesium under these conditions may be completely unacceptable for uses with more severe temperature and/or time requirements.

In order to predict cesium compatibility results for other test conditions, it would be necessary to understand the basic mode of reaction. This would require a study of the true compatibility of cesium with other elements. In the present study, the true compatibility was masked somewhat by other reactions occurring in the test system (e.g., cesium-oxygen reaction, cross contamination, temperature and pressure effects, etc.). A cursory examination of the basic mode of reaction, however, can be made from this study by attempting to distinguish the actual cesium-metal reactions from the other spurious interactions. This method of interpretation separates the major elements studied in this test series into the following categories:

Elements that reacted with cesium	Elements that did not react with cesium
Copper	Tungsten
Zinc	Molybdenum
Gold	Tantalum
Silver	Iron
Aluminum	Nickel
Magnesium	Cobalt
	Platinum

It is noteworthy that all the elements that appeared to be compatible with cesium in this study are transition elements that have unfilled inner electron shells. This correlation suggests that the compatibility of cesium with other materials depends on the particular electron configuration of the base element in the material. Considerably more research (with ultrapure materials over broader test conditions), though, is necessary before the reactiveness of cesium can be understood.

Results for all the materials are shown in table V.

SUMMARY OF RESULTS

A study of the compatibility of cesium vapor with various commercial materials at 500°, 800°, and 1200° F showed that those attacked by cesium vapor to varying degrees were copper, brass, bronze, gold, silver, aluminum, magnesium, Mycalex, Mykroy, and lava. The materials that were not attacked by cesium vapor included tungsten, molybdenum, tantalum, iron, nickel, cobalt, and platinum.

Lewis Research Center
National Aeronautics and Space Administration
Cleveland, Ohio, May 10, 1963

REFERENCES

1. Kirk, R. E. and Othmer, D. F., eds.: Encyclopedia of Chemical Technology. Vol. 1. The Intersci. Encyclopedia, Inc., 1947, pp. 430-455.

2. Mellor, J. W.: A Comprehensive Treatise of Inorganic and Theoretical Chemistry. Vol. II. Longmans, Green and Co., 1946, pp. 419-880.

3. Stuhlinger, E.: Possibilities of Electrical Space Ship Propulsion. Proc. Fifth Int. Astronautical Cong., 1954, pp. 100-119.

4. Mickelsen, William R.: Electric Propulsion for Space Flight. Aero/Space Eng., vol. 19, no. 11, Nov. 1960, pp. 6-11; 36.

5. Thewles, J., Glass, R. C., Hughes, D. J., and Meetham, A. R., eds.: Encyclopaedic Dictionary of Physics. Vol. 3. Pergamon Press, 1961, p. 289.

6. Steg, Leo, and Sutton, George W.: The Prospects of MHD Power Generation. Astronautics, vol. 5, no. 8, Aug. 1960, pp. 22-25; 82-85.

7. Rynn, Nathan, and D'Angelo, Nicola: Device for Generating a Low Temperature, Highly Ionized Cesium Plasma. Rev. Sci. Instr., vol. 31, no. 12, Dec. 1960, pp. 1326-1333.

8. Anon.: Liquid-Metals Handbook. NAVEXOS P-733, Second ed., Atomic Energy Commission and Bur. Ships, Navy Dept., 1952.

9. Petrick, E. N., Husmann, O. K., and Szymanowski, H. W.: Analytical and Experimental Investigation of Compact Charge Ionization. CWR 700-10, Curtiss-Wright Corp., June 1, 1960, pp. 118-146.

10. Anon.: Cesium and Rubidium Metals. Bull. TD-Cs/Rb, Am. Potash and Chem. Corp., 1961.

11. Holley, J. H., Neff, G. R., Weiler, F. B., and Winslow, P. M.: Corrosivity and Contamination of Cesium in Ion Propulsion. Paper Presented at Am. Rocket Soc. Electric Prop. Conf., Berkeley, (Calif.), Mar. 14-16, 1962.

12. Snoke, Donald R., and Lawlor, Patrick J.: Cesium Ion Propellant Feed Systems. Er-4619, Thompson Ramo Wooldridge, Inc., Sept. 1961, pp. 38-92.

13. Wagner, Paul, and Coriell, Sam R.: On the High-Temperature Compatibility of Cesium Gas with Some Dielectrics. Rev. Sci. Instr., vol. 30, no. 10, Oct. 1959, pp. 937-938.

14. Pepkowitz, Leonard P., and Judd, William C.: Determination of Sodium Monoxide in Sodium. Analytical Chem., vol. 22, no. 10, Oct. 1950, pp. 1283-1286.

15. Pepkowitz, L. P., Judd, W. C., and Downer, R. J.: Determination of Sodium Monoxide in Sodium. Analytical Chem., vol. 26, no. 1, Jan. 1954, p. 246.

16. White, J. C., Ross, W. J., and Rowan, Robert, Jr.: Determination of Oxygen in Sodium. Analytical Chem., vol. 26, no. 1, Jan. 1954, pp. 210-212.

17. Anon.: Metals Handbook. Vol. 1. Eighth ed., ASM, 1961.

18. Dayton, B. B.: Relations Between Size of Vacuum Chamber, Outgassing Rate, and Required Pumping Speed. Consolidated Vacuum Corp., Sept. 1959, p. 67.

19. Weatherford, W. D., Jr., Tyler, John C., and Ku, P. M.: Properties of Inorganic Energy-Conversion and Heat-Transfer Fluids for Space Applications. TR 61-96, WADD, Nov. 1961.

20. Tepper, F.: Research and Development of Propellant Feed Systems for Ion Engines. MSA Res. Corp., Callery, (Penn.), Sept. 6, 1961, p. 6.

21. Miller, G. L.: Tantalum and Niobium. Butterworths Sci. Pub., 1959, p. 456.

TABLE I. - SOME PHYSICAL PROPERTIES OF THE ALKALI METALS

[Data from ref. 10.]

	Lithium	Sodium	Potassium	Rubidium	Cesium	Francium
Atomic number	3	11	19	37	55	87
Atomic weight	6.940	22.991	39.10	85.48	132.91	223
Specific heat, at 0° C, cal/(g)(°C)	0.7951	0.292	0.173	0.0802	0.0482	---
Melting point, °C	186	97.7	63.6	39.0	28.45	---
Boiling point, °C	1336	892	774	696	670	---
Ionization potential, v	5.37	5.12	4.32	4.16	3.87	---

TABLE II. - MELTING POINTS AND TYPICAL COMPOSITIONS OF TEST MATERIALS

Material	Approximate melting point, °F	Typical composition, percent
Refractory metals		
Tungsten	6170	99.9 W
Molybdenum	4730	99.9 Mo
Tantalum	5425	99.9 Ta
Iron-base alloys		
1020 Steel (cold rolled)	2790	99.1-99.2 Fe; 0.18-0.23 C; 0.3-0.6 Mn; 0.04 P; 0.05 S
304 Stainless steel	2600	64.9-70.9 Fe; 18-20 Cr; 8-12 Ni; 1 Si; 2 Mn; 0.08 C
Nickel-base alloys		
L-nickel	2620	99.5 Ni; 0.2 Mn; 0.05 Fe; 0.02 Cu; 0.01 C; 0.15 Si; 0.005 S
A-nickel	2635	99.4 Ni; 0.2 Mn; 0.15 Fe; 0.1 Cu; 0.1 C; 0.05 Si; 0.005 S
Inconel X	2550	73.0 Ni; 15.0 Cr; 2.5 Ti; 7 Fe; 1 Cb; 0.9 Al; 0.7 Mn; 0.04 C; 0.3 Si
B-monel	2370 to 2460	67 Ni; 30 Cu; 1.7 Fe; 1.1 Mn; 0.1 C; 0.05 Si; 0.35 S
Copper-base alloys		
Copper (ETP)	1981	99 Cu; 0.04 O_2
Bronze (leaded phosphor bronze)	1910	94 Cu; 5 Sn; 1 Pb
Brass (yellow, Muntz metal)	1710	60 Cu; 40 Zn
Precious metals		
Platinum	3217	99.9 Pt
Gold	1650	99.9 An
Silver	1750	99.9 Ag
Light metals		
Aluminum (Alclad 24ST)	1220	99.9 Al
Magnesium	1202	99.9 Mg
Nonmetals		
Mycalex	----	Glass-bonded mica
Mykroy	----	Glass-bonded mica
Lava	----	Magnesium silicate
Morganite	3670	Aluminum oxide
Sapphire	3670	Aluminum oxide

TABLE III. - ROCKWELL HARDNESS OF TEST SAMPLES

Material	Atmosphere	Test temperature, °F			As-received Rockwell hardness
		500	800	1200	
		Rockwell hardness			
Refractory metals					
Tungsten	Cesium	47	46	46	C-46
	Vacuum	47	47	45	
Molybdenum	Cesium	23	21	22	C-23
	Vacuum	22	22	22	
Iron-base alloys					
1020 Steel	Cesium	20	19	3	C-18
	Vacuum	18	18	5	
304 Stainless steel	Cesium	80	82	77	B-80
	Vacuum	79	81	80	
Nickel-base alloys					
L-nickel	Cesium	54	50	40	B-55
	Vacuum	52	52	43	
A-nickel	Cesium	55	67	43	B-54
	Vacuum	49	48	40	
Inconel X	Cesium	78	81	78	B-79
	Vacuum	78	80	80	
B-monel	Cesium	71	73	66	B-70
	Vacuum	70	72	69	
Copper-base alloys					
Copper	Cesium	87	72	72	B-88
	Vacuum	92	80	73	
Bronze	Cesium	62	26	26	B-69
	Vacuum	58	20	10	
Brass	Cesium	54	17	17	B-60
	Vacuum	52	19	11	
Light metals					
Aluminum	Cesium	30	30	--	B-68
	Vacuum	48	30	--	
Magnesium	Cesium	94	--	--	B-94
	Vacuum	--	--	--	

TABLE IV. - MICROHARDNESS OF TEST SAMPLES

Material	Load,[a] mg	Objective magnification[a]	Atmosphere	Test temperature, °F			As-received hardness
				500	800	1200	
				Diamond-pyramid hardness			
Refractory metals							
Tungsten	100	50	Cesium	500-550	480-540	500-525	500-550
			Vacuum	505-550	475-525	475-535	
Molybdenum	100	50	Cesium	255-280	260-285	260-285	265-285
			Vacuum	255-285	225-280	250-275	
Tantalum	25	50	Cesium	125-140	100-120	260-320	115-130
			Vacuum	115-120	135-160	275-350	
Iron-base alloys							
1020 Steel	100	50	Cesium	225-260	210-240	90-115	220-250
			Vacuum	230-270	225-255	100-110	
304 Stainless steel	100	50	Cesium	140-160	160-180	150-200	130-160
			Vacuum	140-175	140-175	140-160	
Nickel-base alloys							
L-nickel	100	50	Cesium	110-120	100-105	95-110	105-110
			Vacuum	95-105	100-115	85-95	
A-nickel	100	50	Cesium	105-140	105-130	100-125	105-135
			Vacuum	85-100	75-110	90-100	
Inconel X	100	50	Cesium	160-180	155-185	175-185	145-175
			Vacuum	145-175	140-180	150-165	
B-monel	100	50	Cesium	130-155	135-160	130-145	120-140
			Vacuum	120-155	105-150	125-135	
Copper-base alloys							
Copper	100	20	Cesium	50-65	50-75	50-55	60-70
			Vacuum	50-65	40-55	45-60	
Bronze	100	50	Cesium	110-125	75-90	55-75	135-160
			Vacuum	95-125	65-80	55-75	
Brass	100	50	Cesium	105-120	65-90	20-30	105-130
			Vacuum	110-115	70-80	25-30	
Precious metals							
Platinum	25	50	Cesium	50-80	70-100	65-70	65-80
			Vacuum	75-80	65-85	60-65	
Silver	25	50	Cesium	45-55	40-45	25-40	35-50
			Vacuum	35-45	45-60	35-40	
Gold	25	50	Cesium	40-50	45-50	35-40	55-65
			Vacuum	35-45	25-35	40-45	
Light metals							
Aluminum	50	20	Cesium	75-85	67-75	-------	130-150
			Vacuum	50-85	75-85	-------	
Magnesium	100	20	Cesium	50-60	45-60	-------	45-55
			Vacuum	-------	-------	-------	

[a]Used in obtaining diamond-pyramid hardness.

TABLE V. - COMPATIBILITY OF VARIOUS MATERIALS WITH CESIUM

Material	Cesium attack at temperatures of 500°, 800°, and 1200° F	Remarks
Refractory metals		
Tungsten	No	
Molybdenum	No	
Tantalum	No	Susceptible to embrittlement by interstitial contaminants at 1200° F
Iron-base alloys		
1020 Steel	No	Recrystallization and softening at 1200° F
304 Stainless steel	No	Recrystallization and softening at 1200° F
Nickel-base alloys		
L-nickel	No	Solution of grain-boundary precipitates at all temperatures
A-nickel	No	Solution of precipitates and grain growth at all temperatures
Inconel X	No	Vaporization of precipitates from surface zone at all temperatures
B-monel	No	Vaporization of alloy constituents at all temperatures
Copper-base alloys		
Copper	Yes	Moderate attack of surface
Bronze	Yes	Moderate attack of surface
Brass	Yes	Dezincification and gross grain-boundary attack
Precious metals		
Platinum	No	
Gold	Yes	Considerable surface attack, particularly at 800° F; extreme grain growth at all temperatures
Silver	Yes	Severe grain-boundary attack and extreme grain growth at all temperatures
Light metals		
Aluminum	Yes	Gross attack of both core and clad at 500° and 800° F (melts near 1200° F)
Magnesium	Yes	Severe attack of grain boundaries at 500° and 800° F (melts below 1200° F)
Nonmetals		
Mycalex	Yes	Sample laminated at 1200° F; slight reaction at all temperatures
Mykroy	Yes	Slight reaction at all temperatures
Lava	Yes	Gross attack of sample core at all temperatures
Morganite	No	
Sapphire	No	

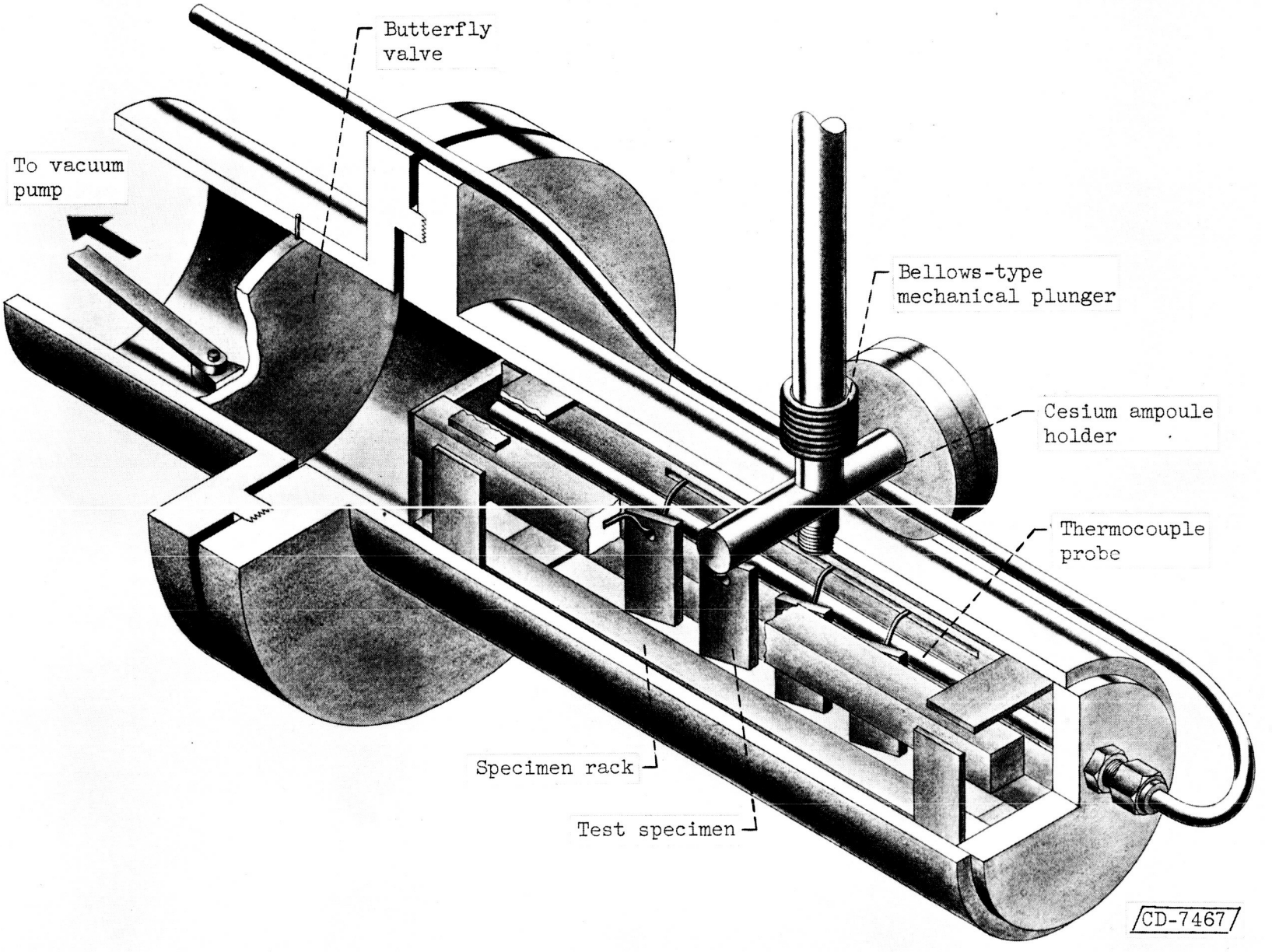

Figure 1. - Test chamber used in cesium-compatability studies.

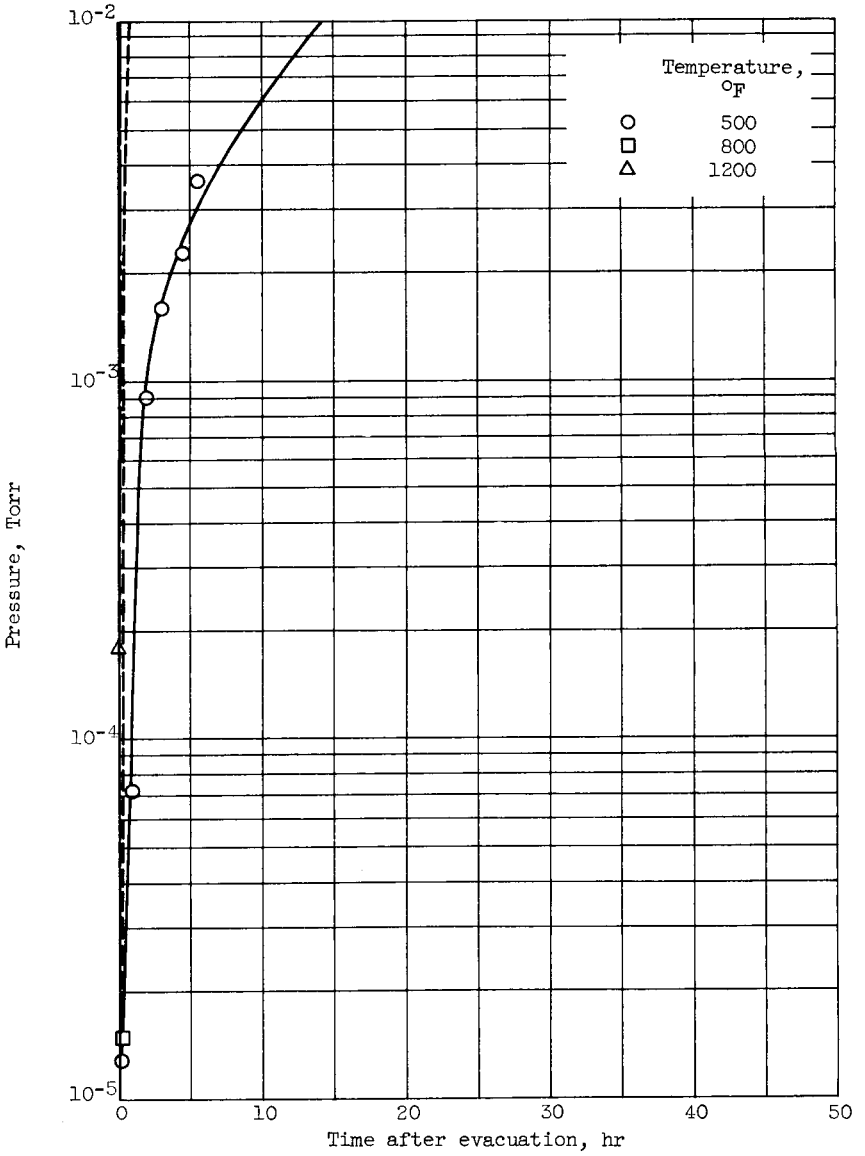

(a) Pressure, 10^{-5} to 10^{-2} Torr.

Figure 2. - Pressure rise in test chamber at indicated temperatures with pumping system closed off.

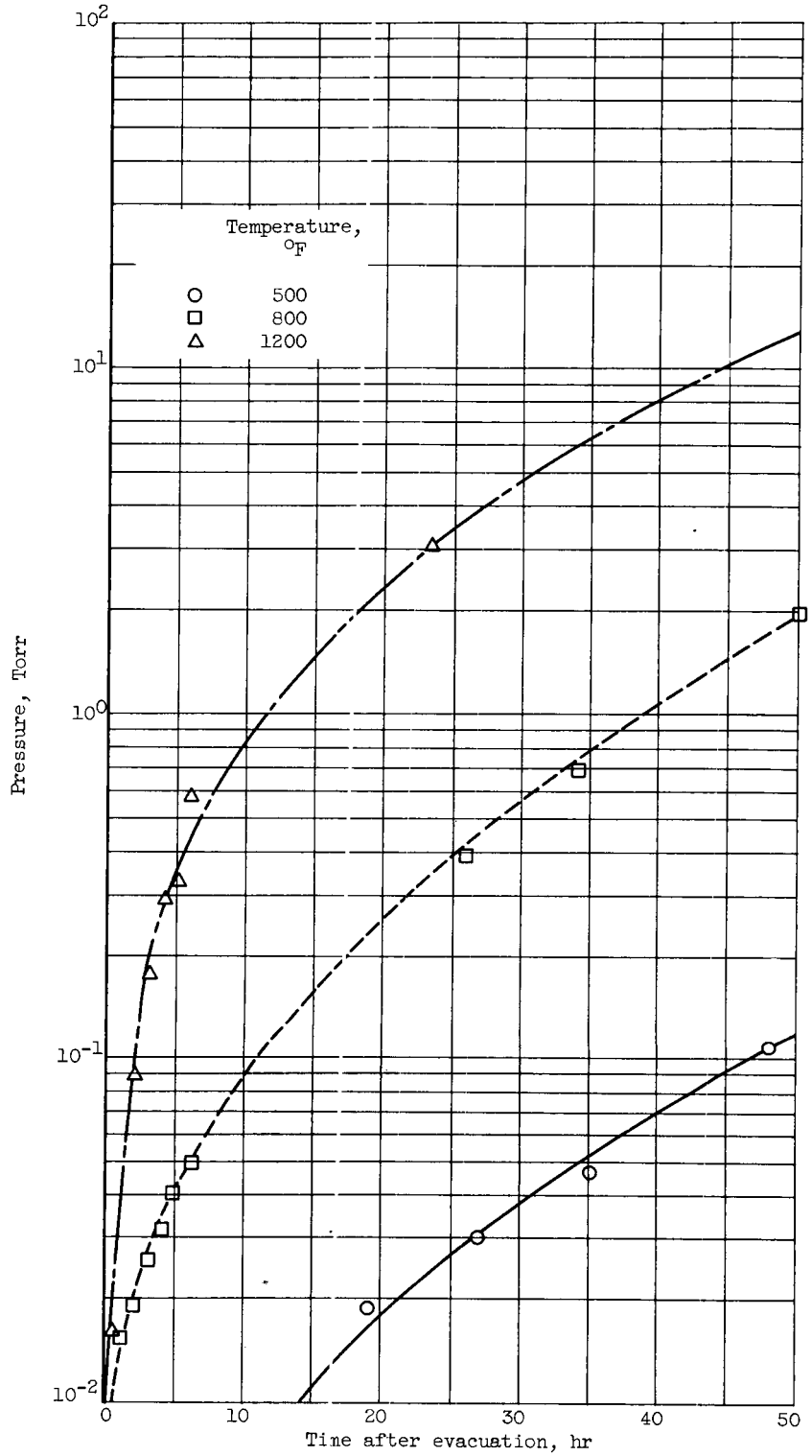

(b) Pressure, 10^{-2} to 10^2 Torr.

Figure 2. - Concluded. Pressure rise in test chamber at indicated temperatures with pumping system closed off.

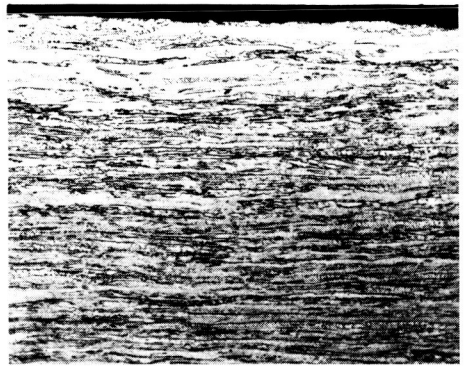

(a) Starting material.

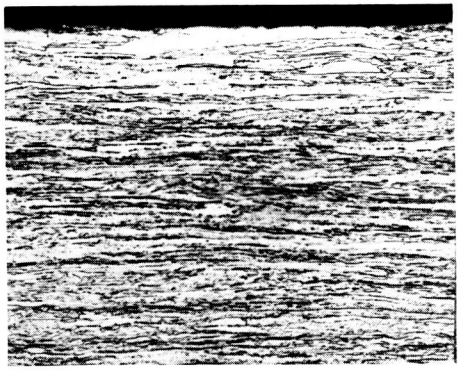

(b) At 500° F in vacuum.

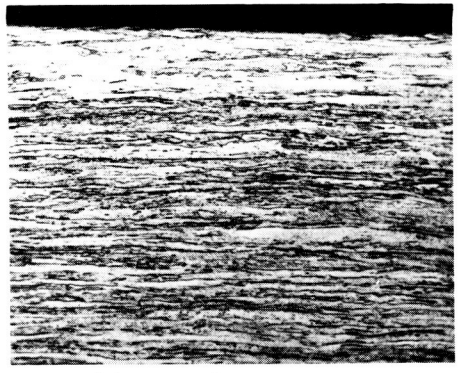

(c) At 800° F in vacuum.

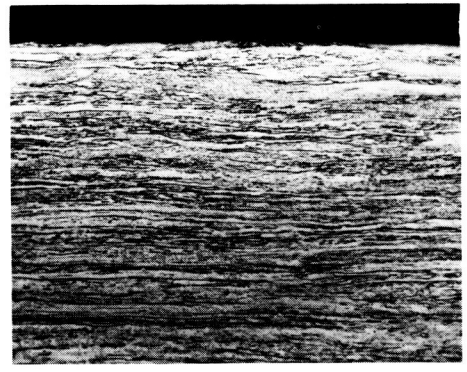

(d) At 1200° F in vacuum.

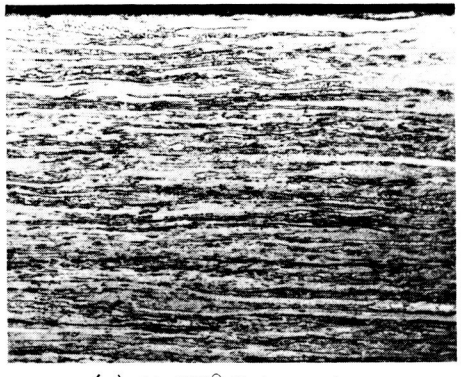

(e) At 500° F in cesium.

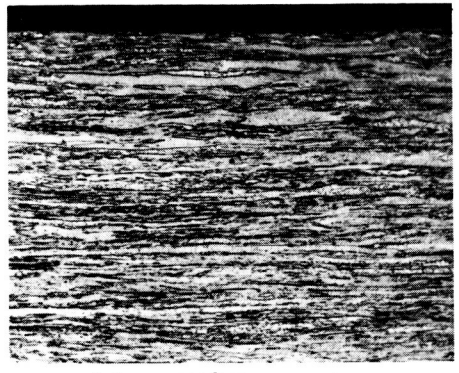

(f) At 800° F in cesium.

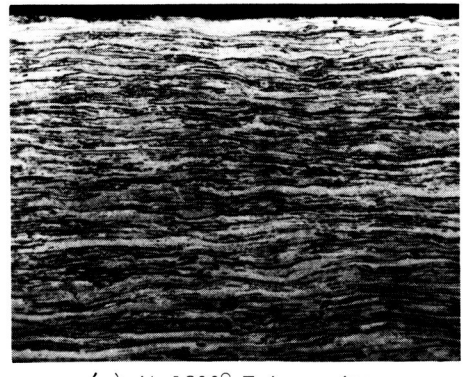

(g) At 1200° F in cesium.

Figure 3. - Photomicrographs of tungsten tested for 48 hours. Etch, potassium hydroxide plus potassium ferricyanide. ×250.

C-64623

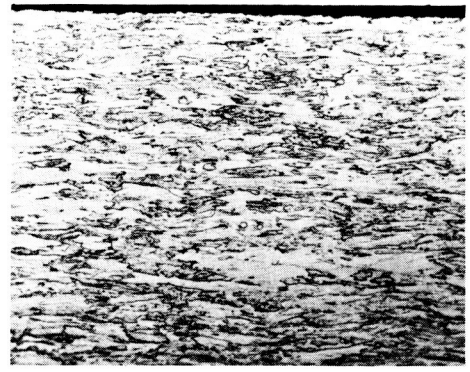

(a) Starting material.

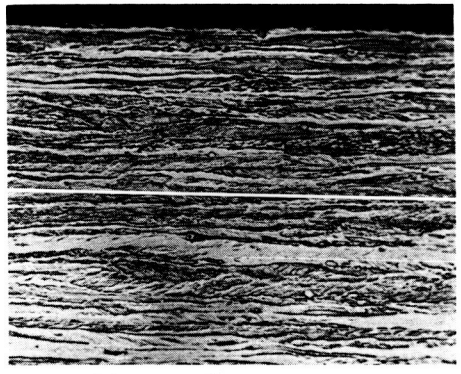

(b) At 500° F in vacuum.

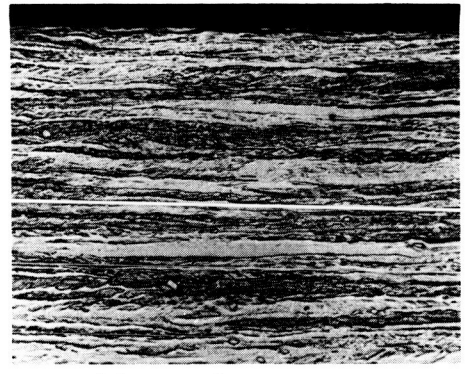

(c) At 800° F in vacuum.

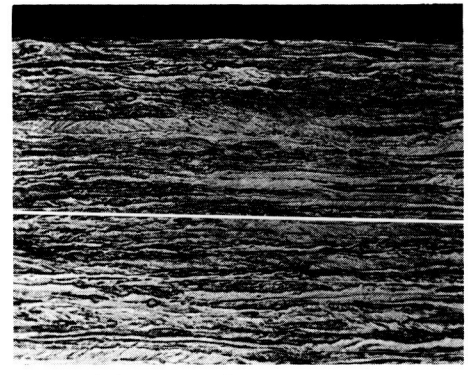

(d) At 1200° F in vacuum.

(e) At 500° F in cesium.

(f) At 800° F in cesium.

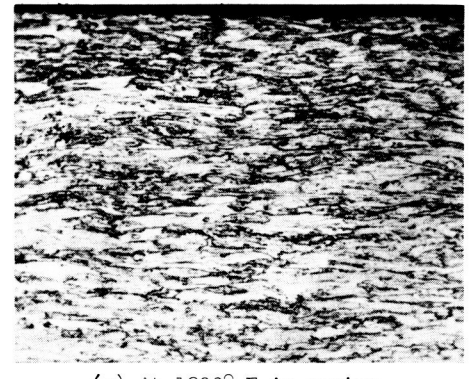

(g) At 1200° F in cesium.

Figure 4. - Photomicrographs of molybdenum tested for 48 hours. Etch, potassium hydroxide plus potassium ferricyanide. ×250.

C-64624

(a) Starting material.

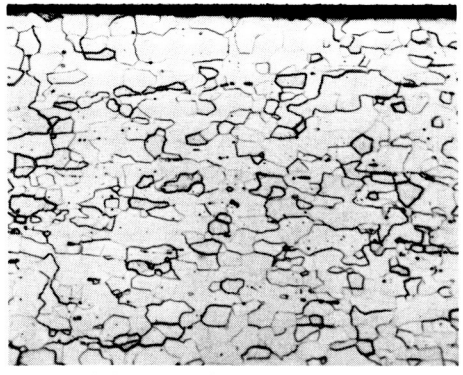

(b) At 500° F in vacuum.

(c) At 800° F in vacuum.

(d) At 1200° F in vacuum.

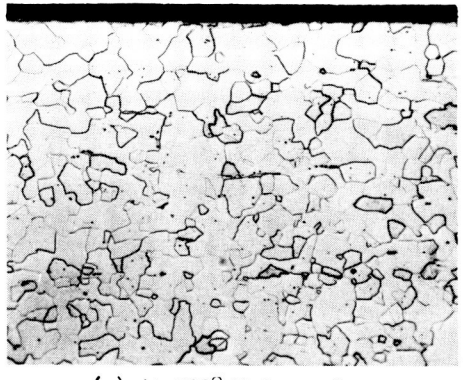

(e) At 500° F in cesium.

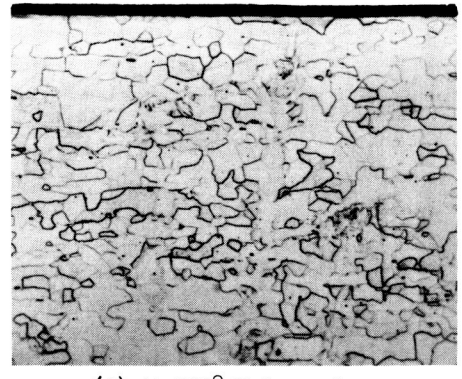

(f) At 800° F in cesium.

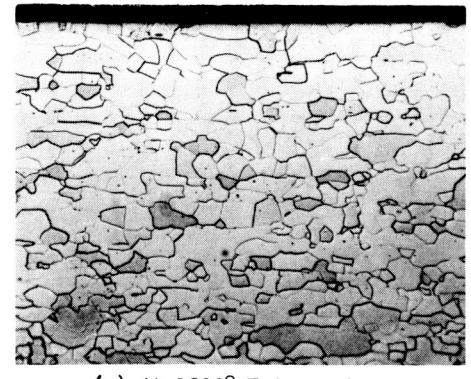

(g) At 1200° F in cesium.

Figure 5. - Photomicrographs of tantalum tested for 48 hours. Etch, ammonium fluoride plus hydrofluoric acid. ×250.

C-64625

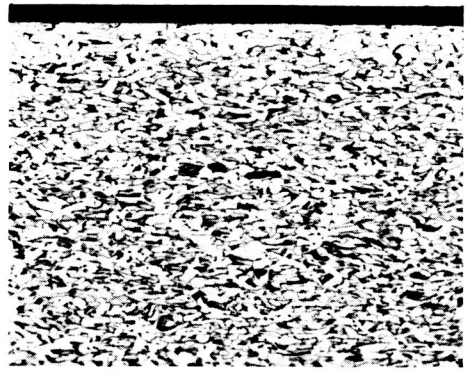

(a) Starting material.

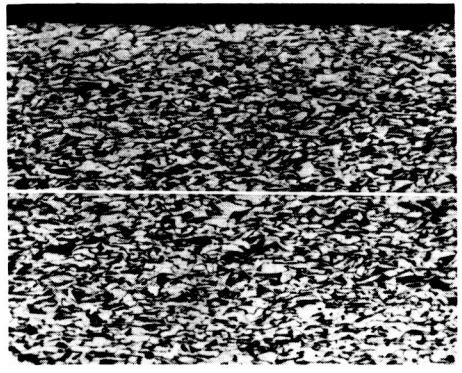

(b) At 500° F in vacuum.

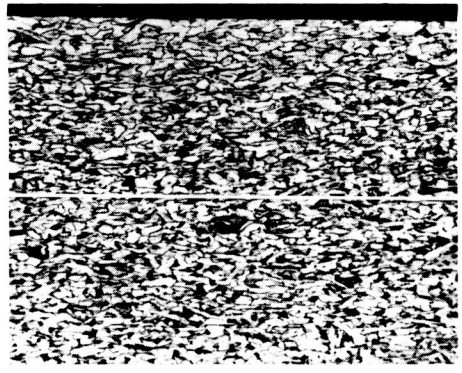

(c) At 800° F in vacuum.

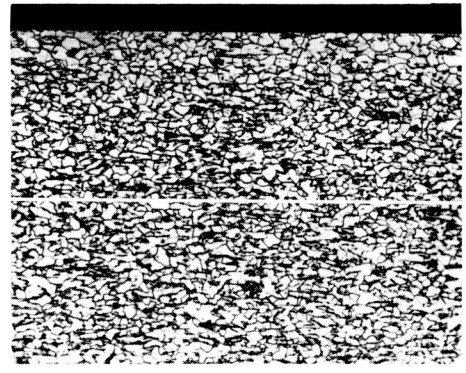

(d) At 1200° F in vacuum.

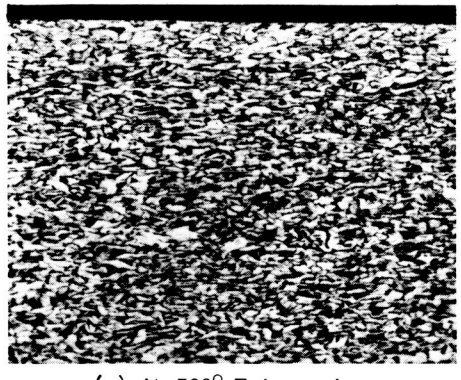

(e) At 500° F in cesium.

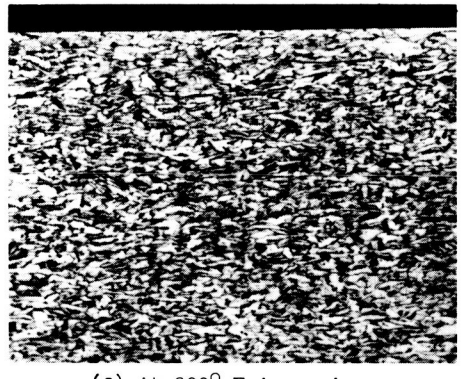

(f) At 800° F in cesium.

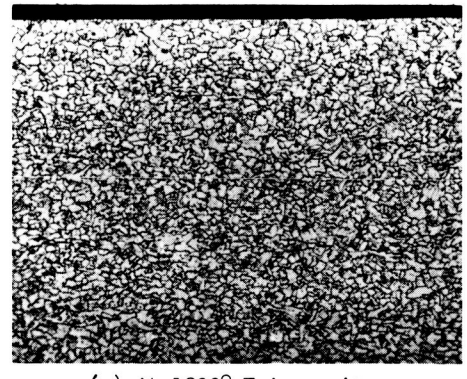

(g) At 1200° F in cesium.

Figure 6. - Photomicrographs of 1020 steel (cold rolled) tested for 48 hours. Etch, 2 percent nital. ×150.
C-64626

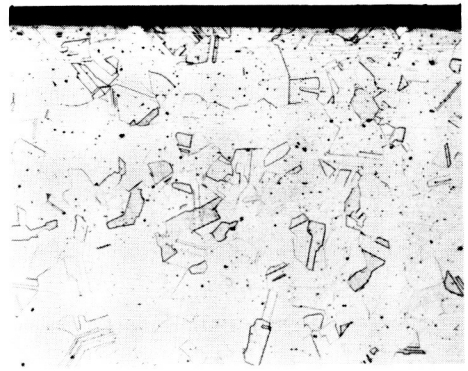

(a) Starting material.

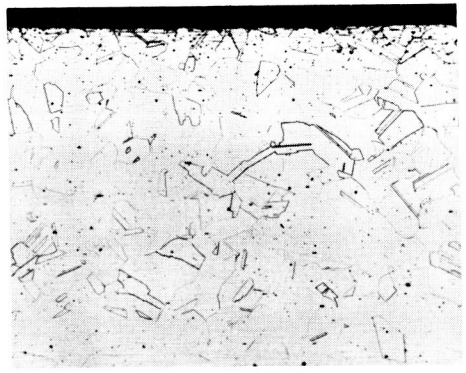

(b) At 500° F in vacuum.

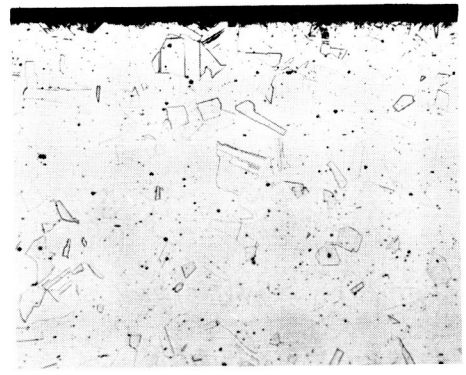

(c) At 800° F in vacuum.

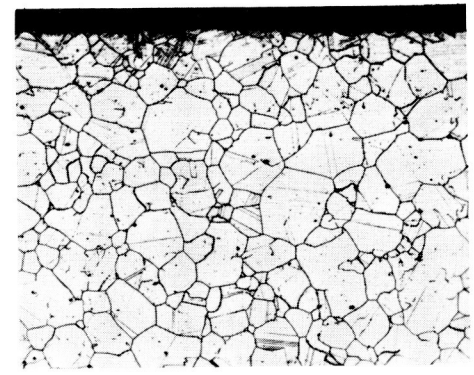

(d) At 1200° F in vacuum.

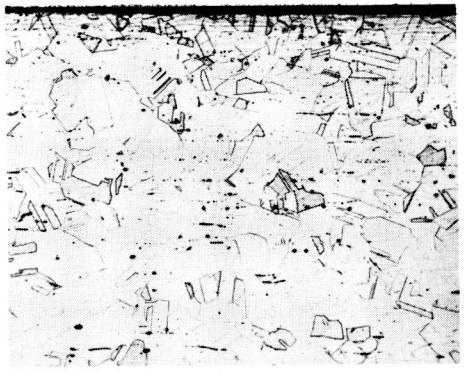

(e) At 500° F in cesium.

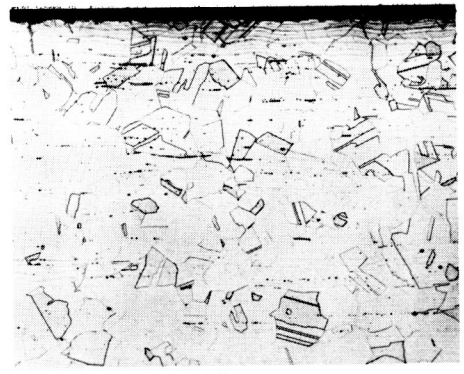

(f) At 800° F in cesium.

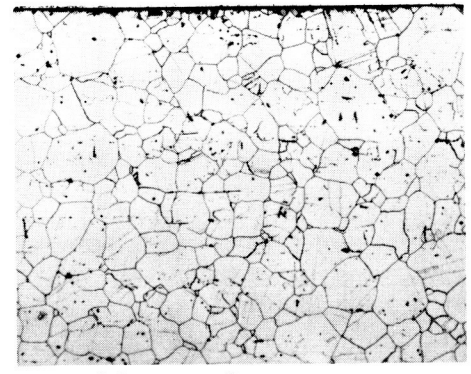

(g) At 1200° F in cesium.

Figure 7. - Photomicrographs of 304 stainless steel tested for 48 hours. Etch, 10 percent ammonium persulfate. ×150.
C-64627

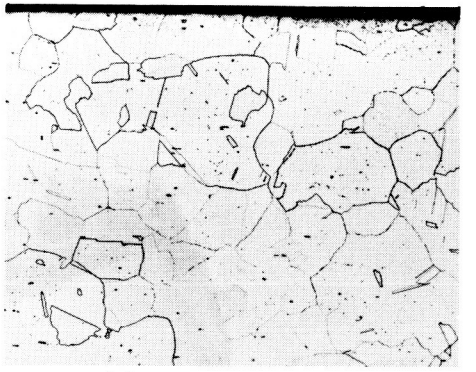

(a) Starting material.

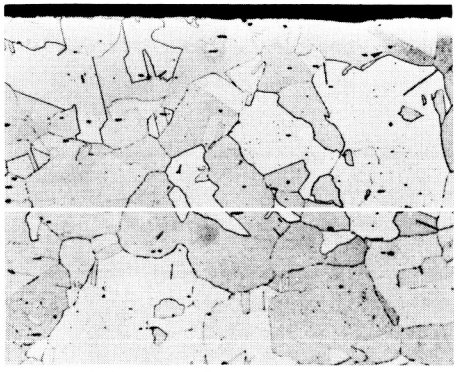

(b) At 500° F in vacuum.

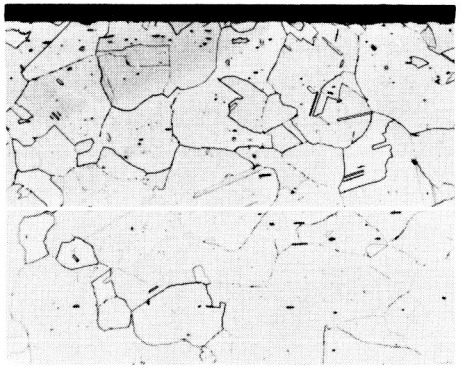

(c) At 800° F in vacuum.

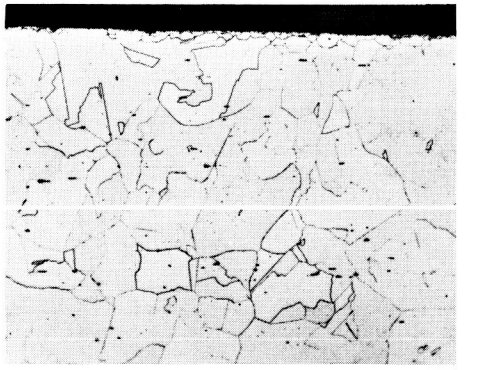

(d) At 1200° F in vacuum.

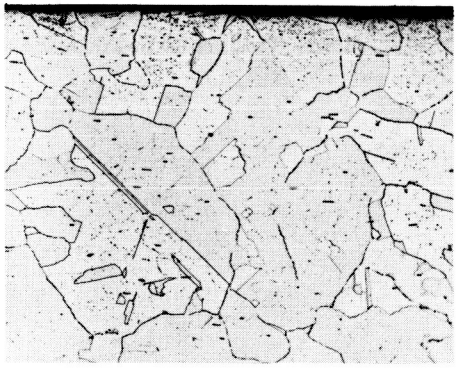

(e) At 500° F in cesium.

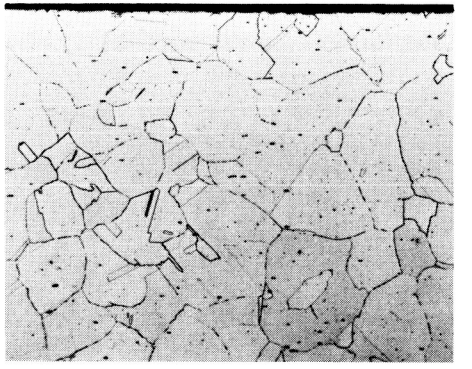

(f) At 800° F in cesium.

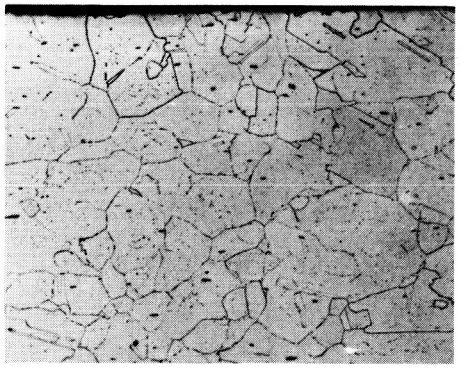

(g) At 1200° F in cesium.

Figure 8. - Photomicrographs of L-nickel tested for 48 hours. Etch, 10 percent potassium cyanide plus 10 percent ammonium persulfate. ×150.

C-64628

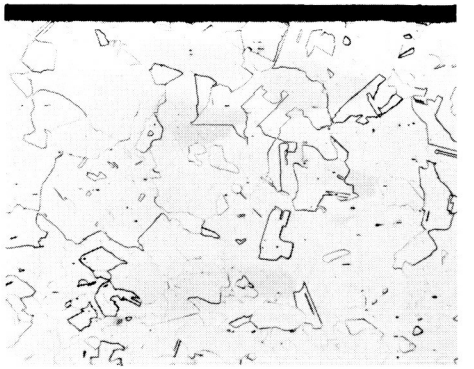

(a) Starting material.

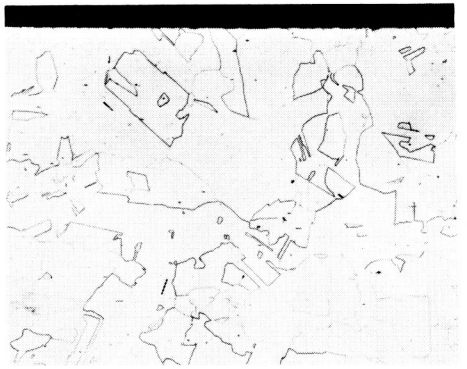

(b) At 500° F in vacuum.

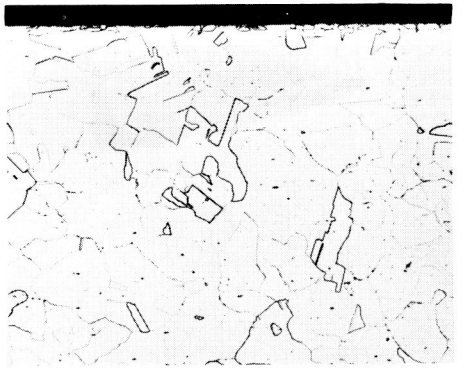

(c) At 800° F in vacuum.

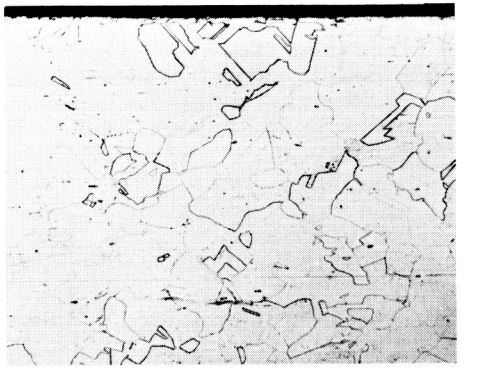

(d) At 1200° F in vacuum.

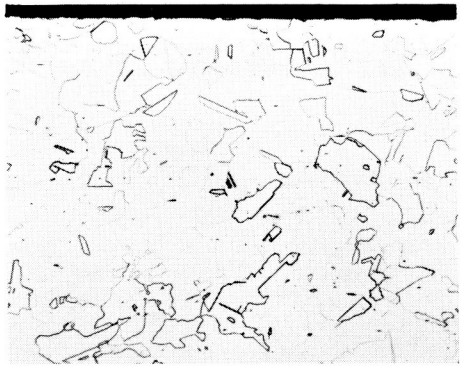

(e) At 500° F in cesium.

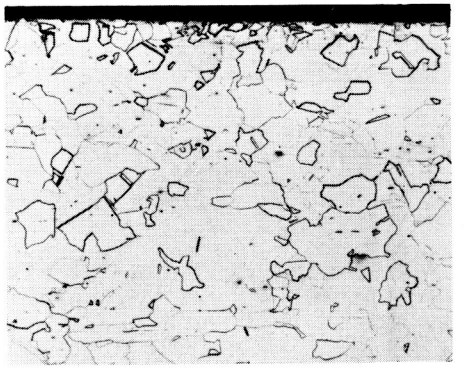

(f) At 800° F in cesium.

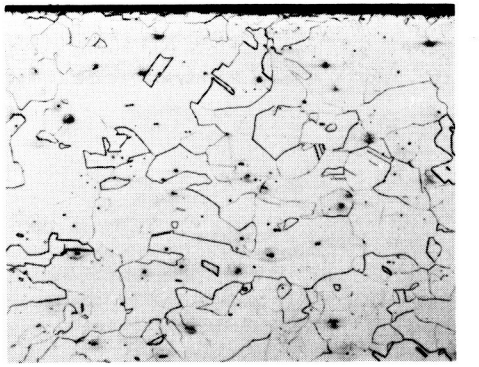

(g) At 1200° F in cesium.

Figure 9. - Photomicrographs of A-nickel tested for 48 hours. Etch, hydrochloric acid plus nitric acid plus sulfuric acid. X150.

C-64629

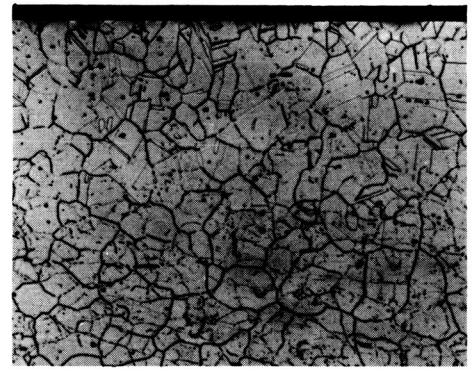

(a) Starting material.

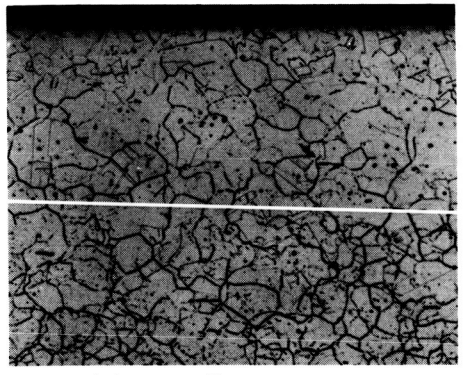

(b) At 500° F in vacuum.

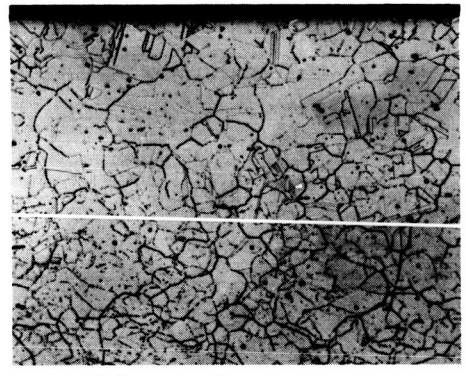

(c) At 800° F in vacuum.

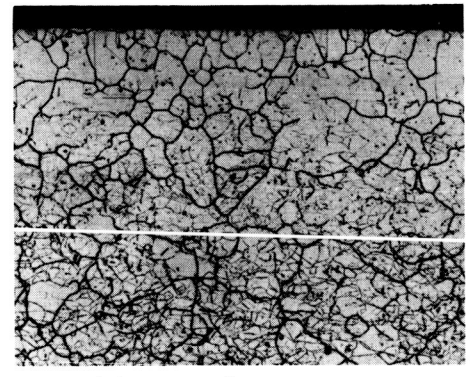

(d) At 1200° F in vacuum.

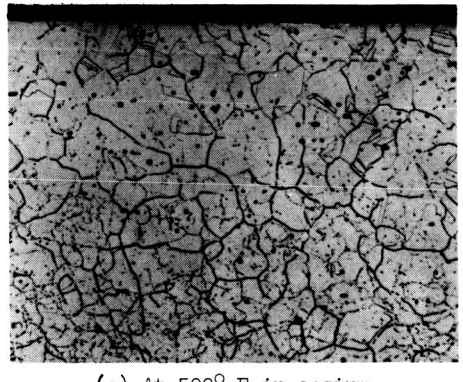

(e) At 500° F in cesium.

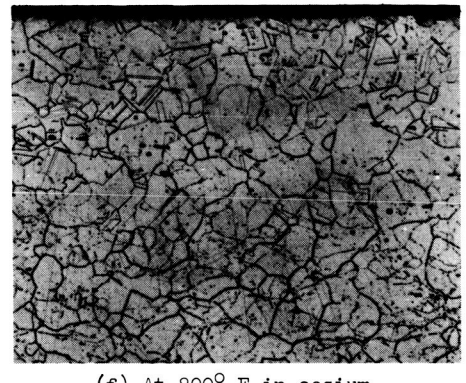

(f) At 800° F in cesium.

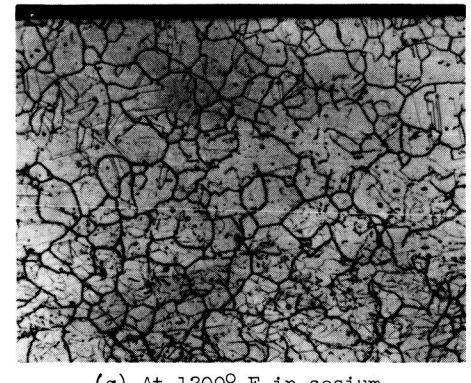

(g) At 1200° F in cesium.

Figure 10. - Photomicrographs of Inconel X tested for 48 hours. Etch, 10 percent oxalic acid. ×200.
C-64630

(a) Starting material.

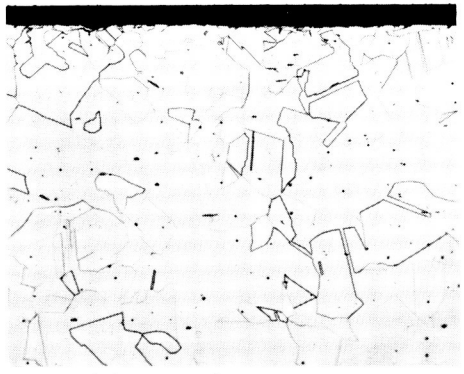

(b) At 500° F in vacuum.

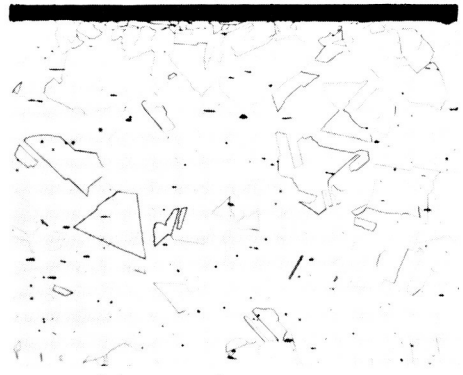

(c) At 800° F in vacuum.

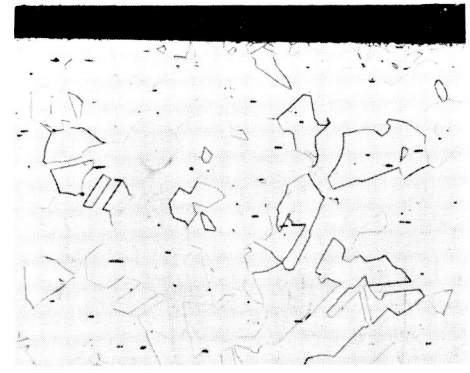

(d) At 1200° F in vacuum.

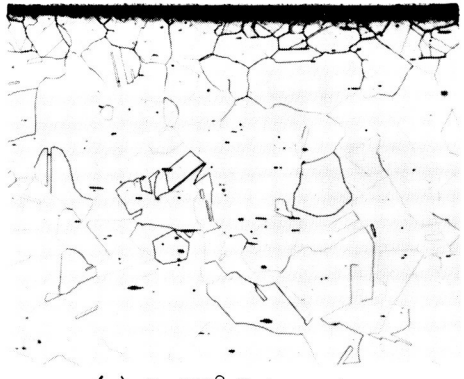

(e) At 500° F in cesium.

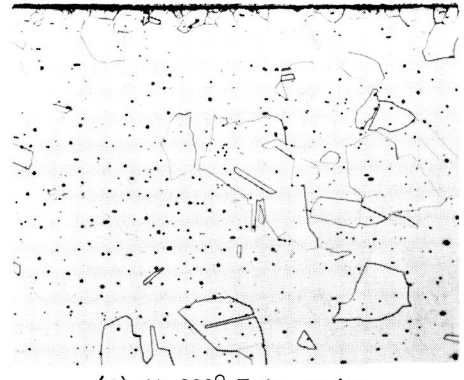

(f) At 800° F in cesium.

(g) At 1200° F in cesium.

Figure 11. - Photomicrographs of B-monel tested for 48 hours. Etch, 10 percent ammonium persulfate. ×150.
C-64631

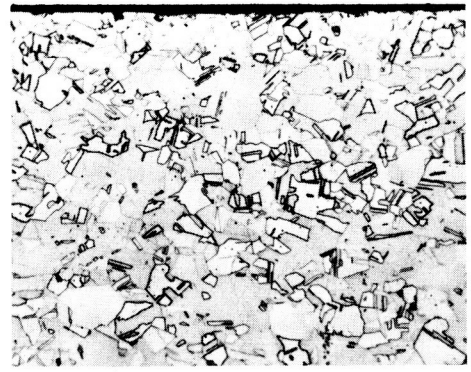

(a) Starting material.

(b) At 500° F in vacuum.

(c) At 800° F in vacuum.

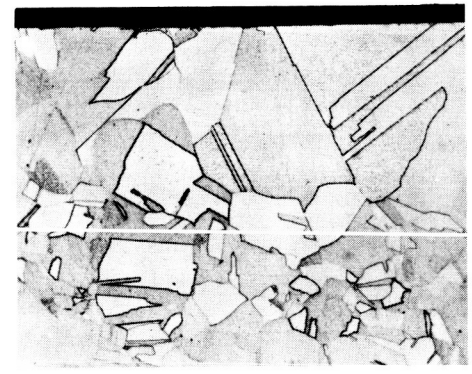

(d) At 1200° F in vacuum.

(e) At 500° F in cesium.

(f) At 800° F in cesium.

(g) At 1200° F in cesium.

Figure 12. - Photomicrographs of copper tested for 48 hours. Etch, 10 percent ammonium persulfate. ×250.
C-64632

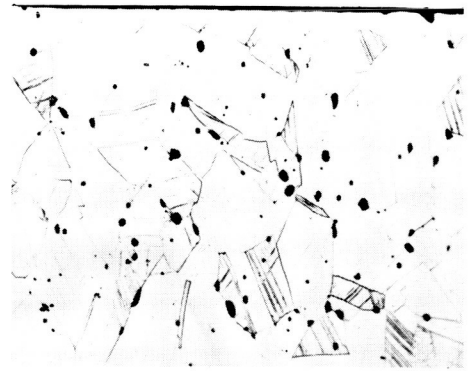

(a) Starting material.

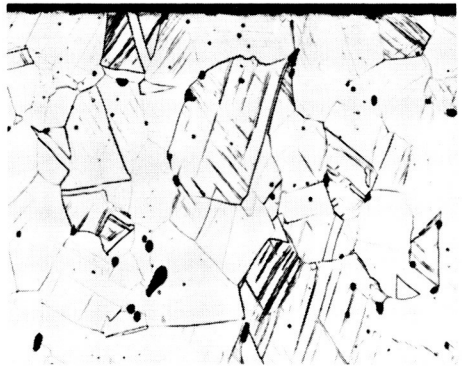

(b) At 500° F in vacuum.

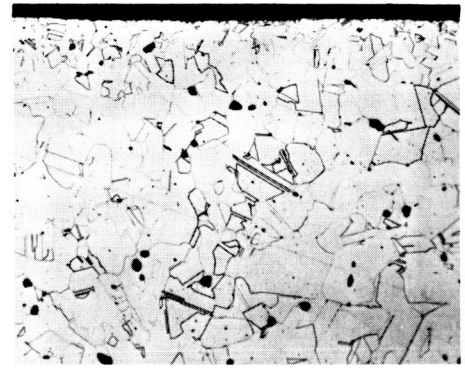

(c) At 800° F in vacuum.

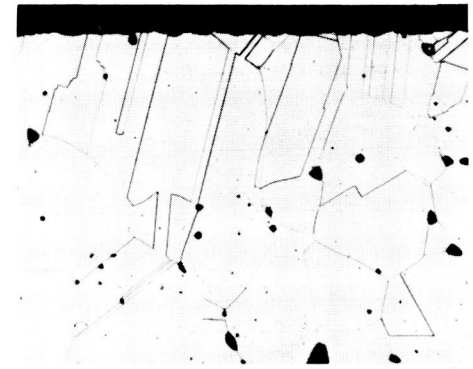

(d) At 1200° F in vacuum.

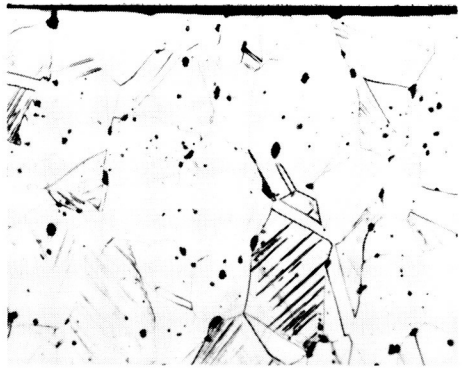

(e) At 500° F in cesium.

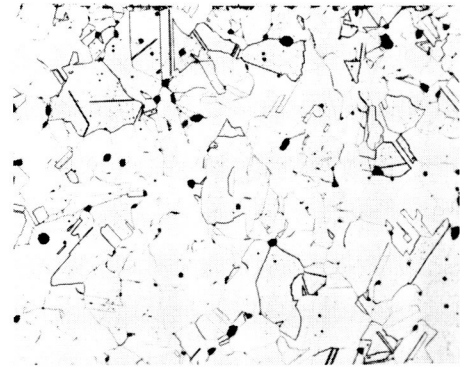

(f) At 800° F in cesium.

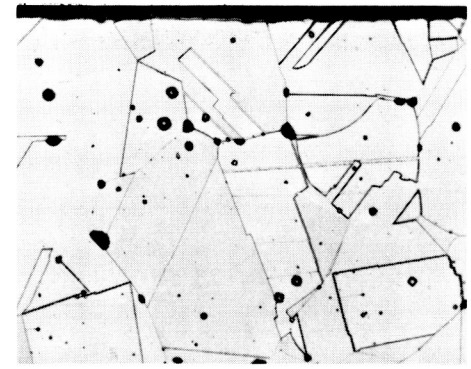

(g) At 1200° F in cesium.

Figure 13. - Photomicrographs of bronze tested for 48 hours. Etch, 10 percent ammonium persulfate. ×250.
C-64633

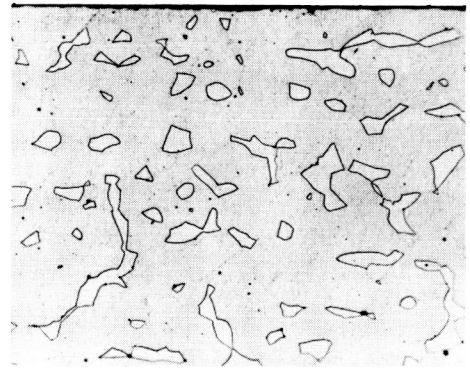

(a) Starting material.

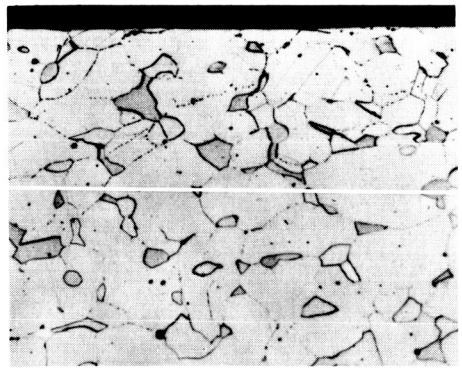

(b) At 500° F in vacuum.

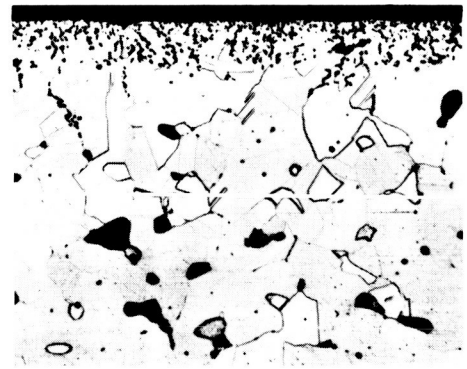

(c) At 800° F in vacuum.

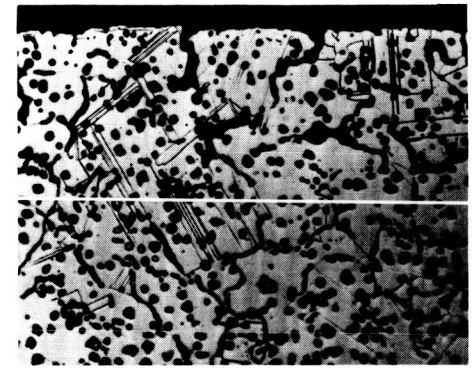

(d) At 1200° F in vacuum.

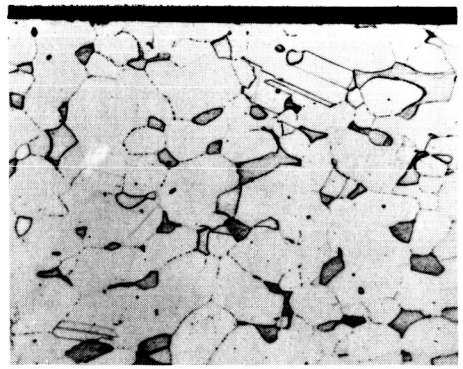

(e) At 500° F in cesium.

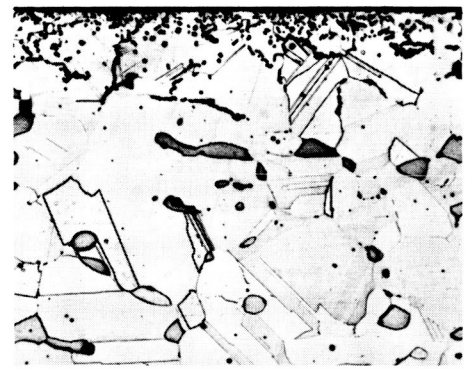

(f) At 800° F in cesium.

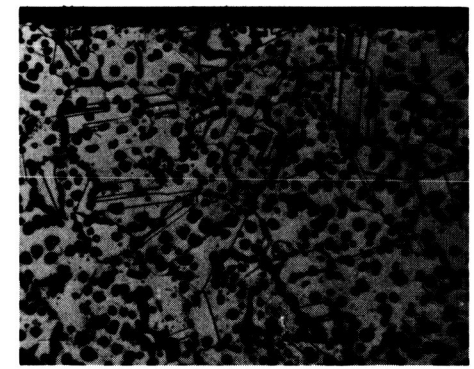

(g) At 1200° F in cesium.

Figure 14. - Photomicrographs of brass tested for 48 hours. Etch, 10 percent ammonium persulfate. ×250.
C-64634

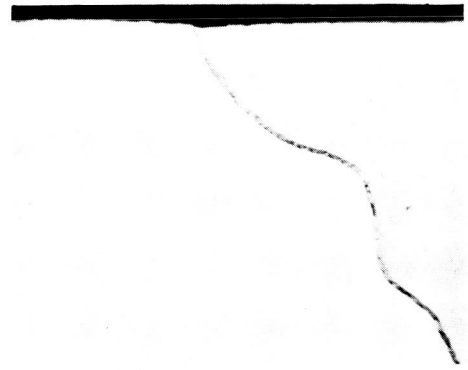

(a) Starting material.

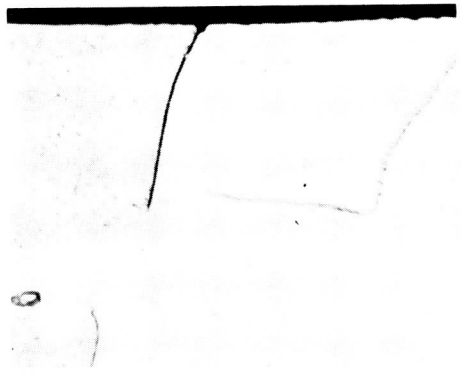

(b) At 500° F in vacuum.

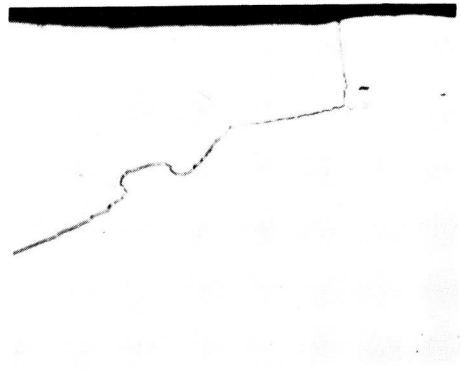

(c) At 800° F in vacuum.

(d) At 1200° F in vacuum.

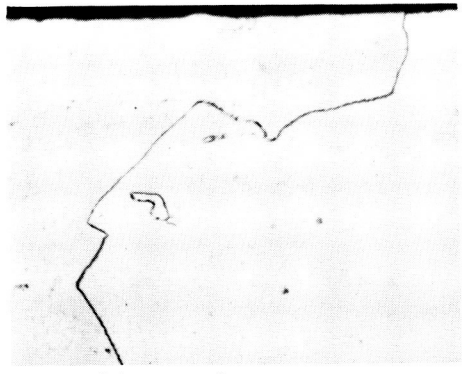

(e) At 500° F in cesium.

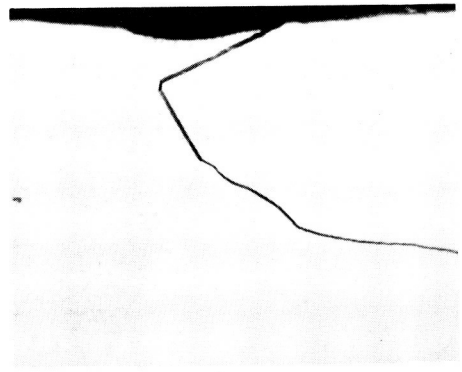

(f) At 800° F in cesium.

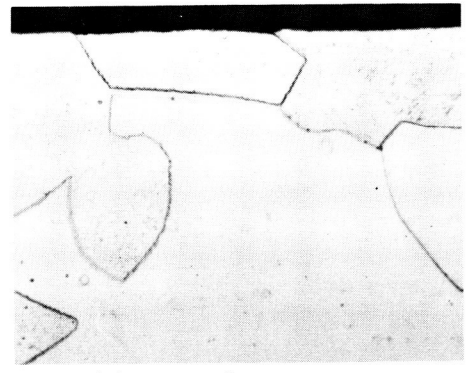

(g) At 1200° F in cesium.

Figure 15. - Photomicrographs of platinum tested for 48 hours. Etch, aqua regia. ×750.
C-64635

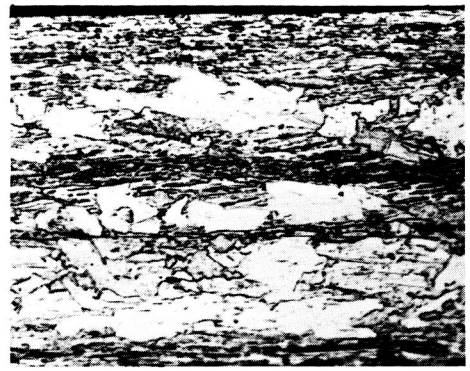

(a) Starting material.

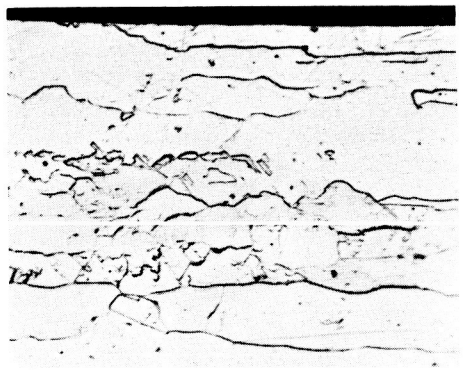

(b) At 500° F in vacuum.

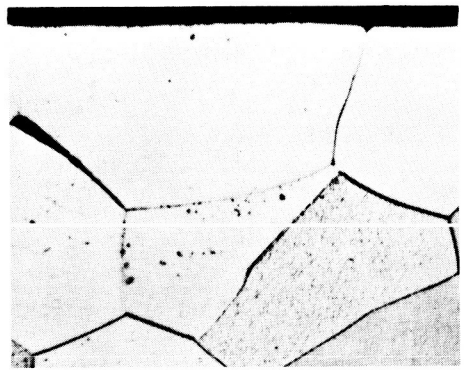

(c) At 800° F in vacuum.

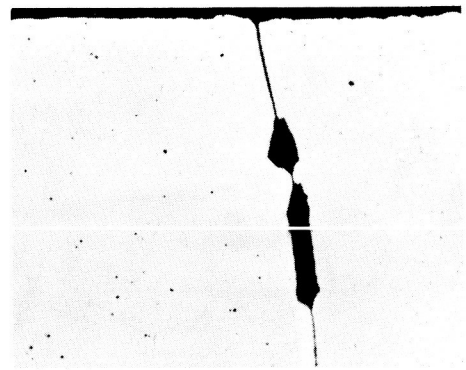

(d) At 1200° F in vacuum.

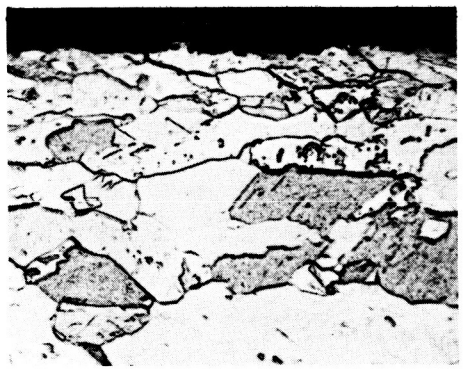

(e) At 500° F in cesium.

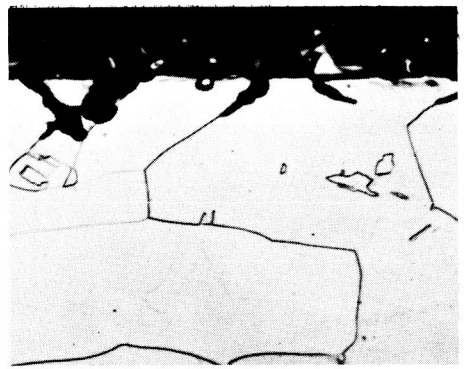

(f) At 800° F in cesium.

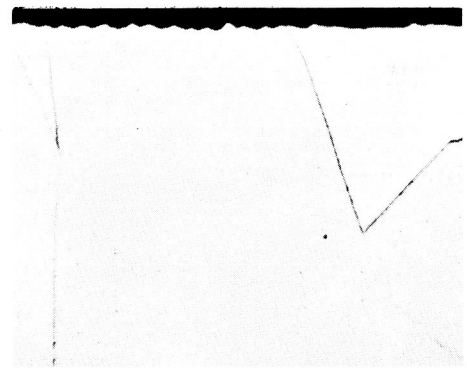

(g) At 1200° F in cesium.

Figure 16. - Photomicrographs of gold tested for 48 hours. Etch, aqua regia. X750.
C-64636

(a) Starting material.

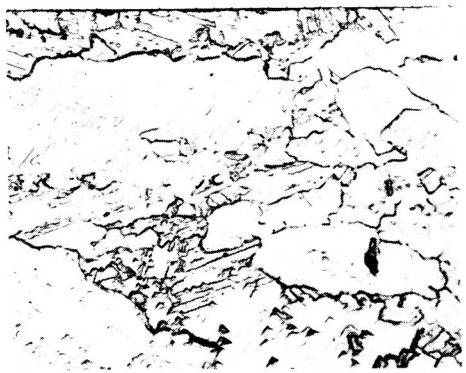

(b) At 500° F in vacuum.

(c) At 800° F in vacuum.

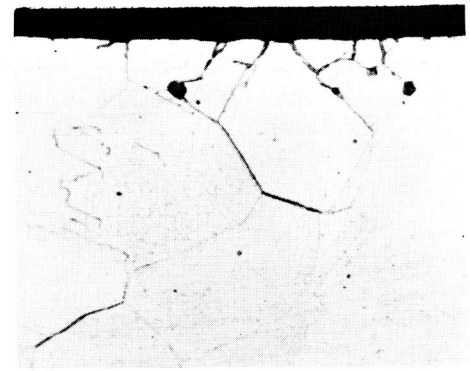

(d) At 1200° F in vacuum.

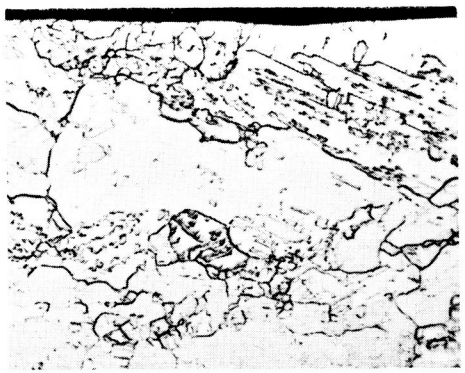

(e) At 500° F in cesium.

(f) At 800° F in cesium.

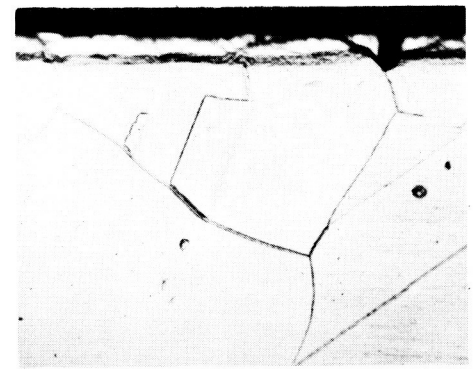

(g) At 1200° F in cesium.

Figure 17. - Photomicrographs of silver tested for 48 hours. Etch, ammonium hydroxide plus hydrogen peroxide. ×750.
C-64637

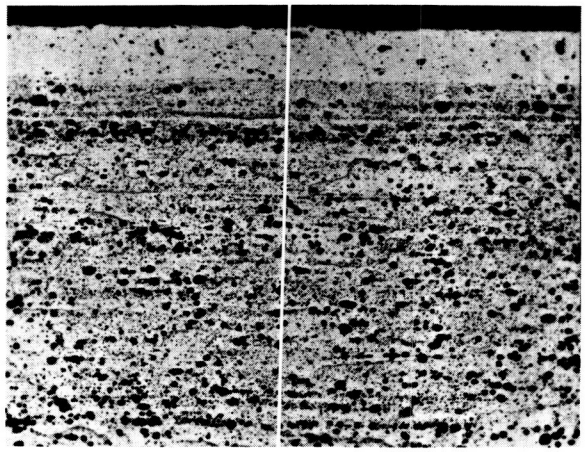

(a) Starting material.

(b) At 500° F in vacuum.

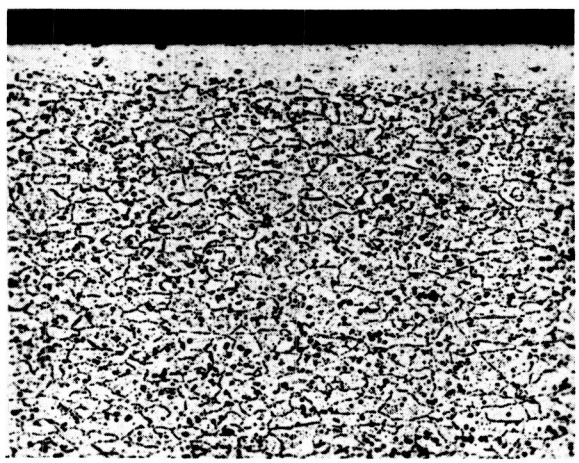

(c) At 800° F in vacuum.

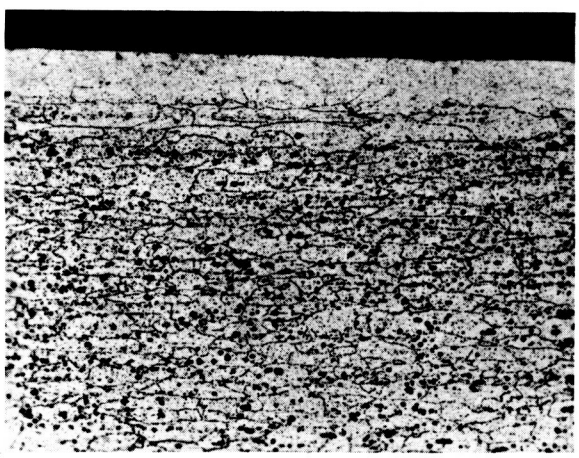

(d) At 500° F in cesium.

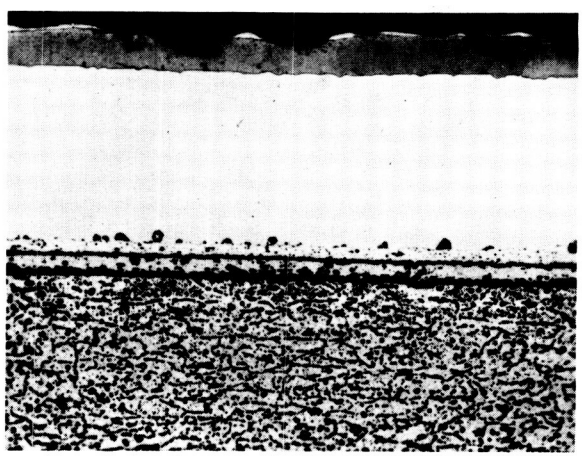

(e) At 800° F in cesium.

Figure 18. - Photomicrographs of aluminum tested for 48 hours at 500° and 800° F. Etch, 10 percent ammonium persulfate. X150.

C-64638

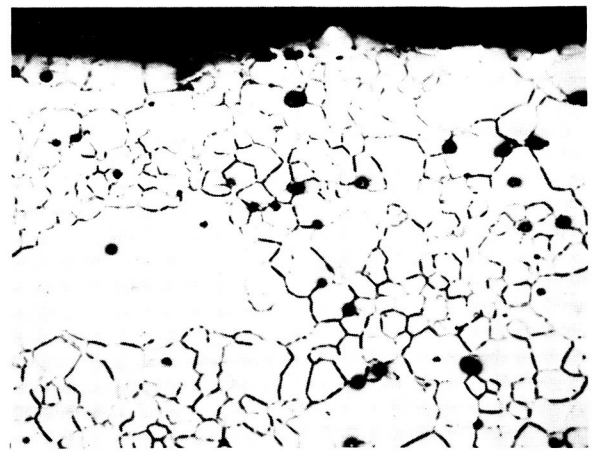

(a) Starting material.

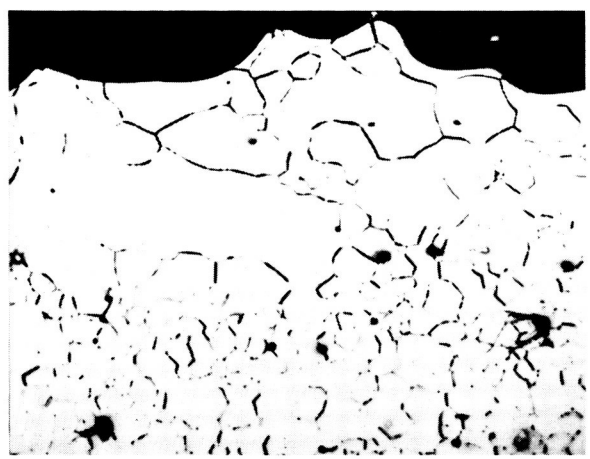

(b) At 500° F in cesium.

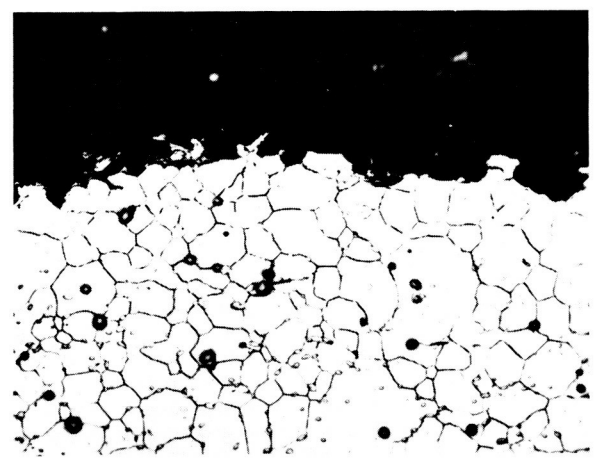

(c) At 800° F in cesium.

Figure 19. - Photomicrographs of magnesium tested for 48 hours at 500° and 800° F in cesium. Etch, ethylene glycol plus nitric acid plus hydrogen peroxide. ×250. C-64639

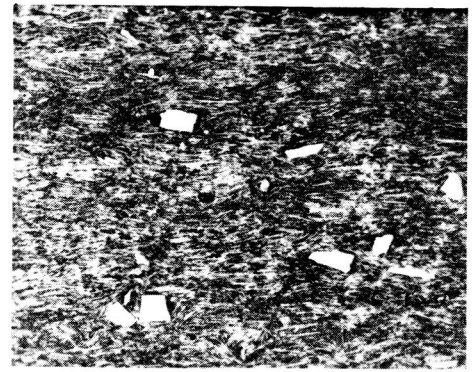

(a) Starting material.

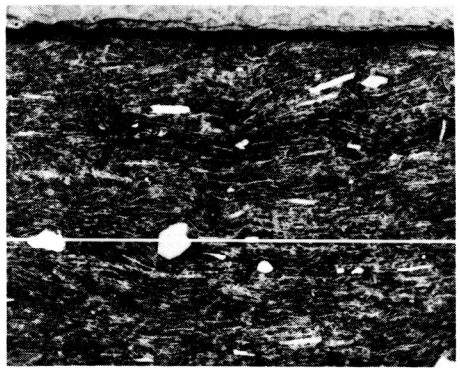

(b) At 500° F in vacuum.

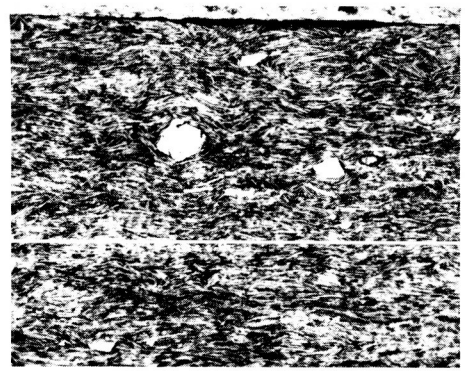

(c) At 800° F in vacuum.

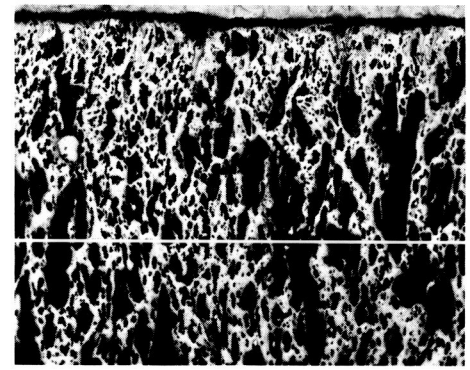

(d) At 1200° F in vacuum.

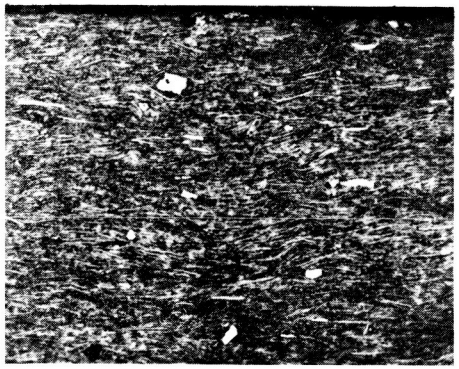

(e) At 500° F in cesium.

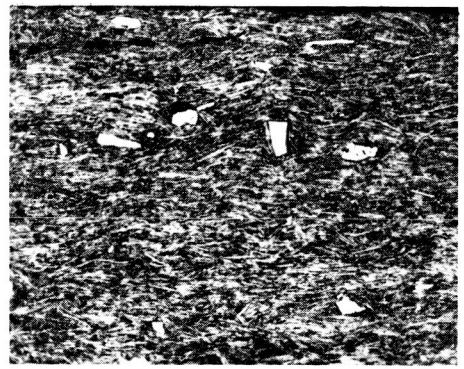

(f) At 800° F in cesium.

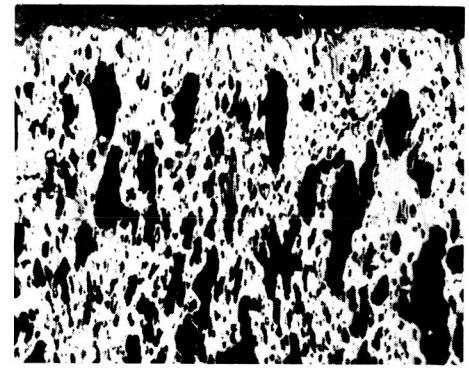

(g) At 1200° F in cesium.

Figure 20. - Photomicrographs of Mycalex tested for 48 hours. Etch, nitric acid plus hydrofluoric acid. ×100.
C-64640

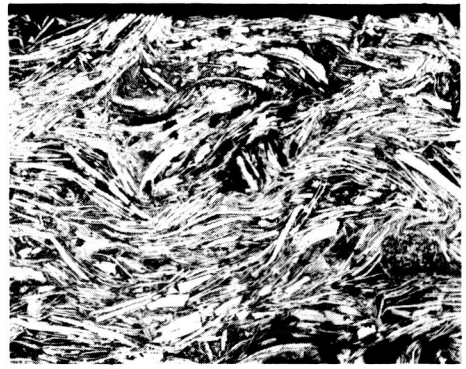

(a) Starting material.

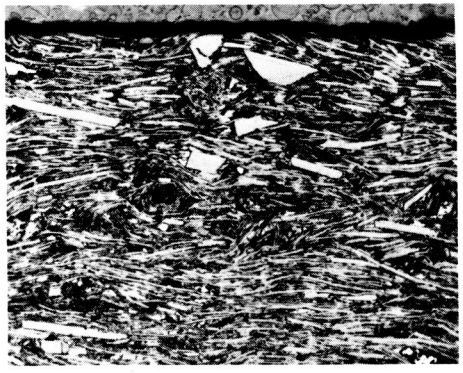

(b) At 500° F in vacuum.

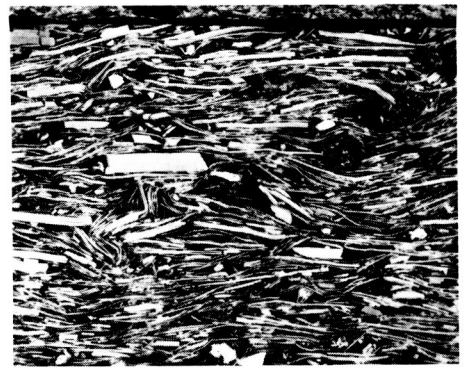

(c) At 800° F in vacuum.

(d) At 1200° F in vacuum.

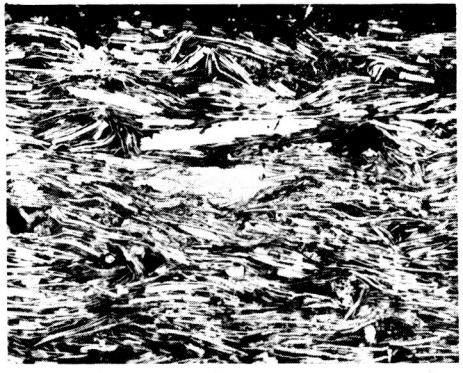

(e) At 500° F in cesium.

(f) At 800° F in cesium.

(g) At 1200° F in cesium.

Figure 21. - Photomicrographs of Mykroy tested for 48 hours. Etch, lactic acid plus nitric acid plus hydrofluoric acid. ×100.

C-64641

(a) Starting material.

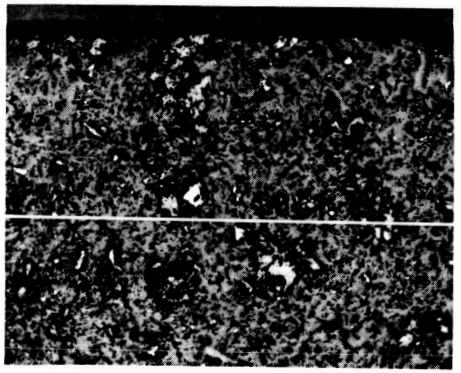

(b) At 500° F in vacuum.

(c) At 800° F in vacuum.

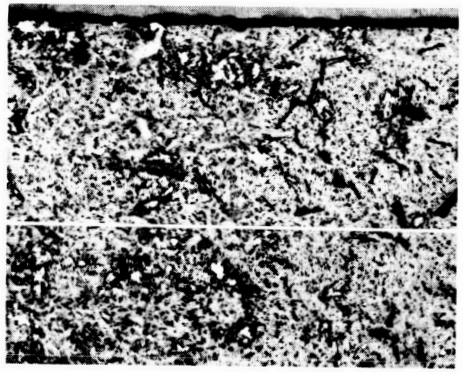

(d) At 1200° F in vacuum.

(e) At 500° F in cesium.

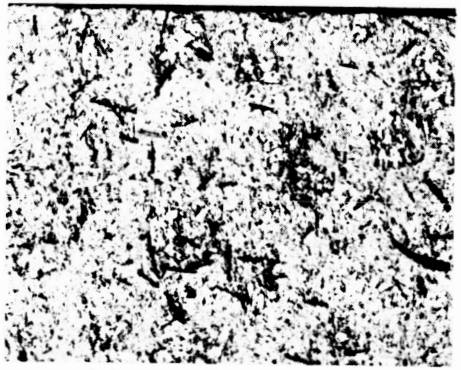

(f) At 800° F in cesium.

(g) At 1200° F in cesium.

Figure 22. - Photomicrographs of lava tested for 48 hours. No etch. ×100.
C-64642